Synthesis and Evaluation of Bifunctional sGC Regulators: Optimization of a Connecting Linker

ARTICLE *in* JOURNAL OF MEDICINAL CHEMISTRY · AUGUST 2013

Impact Factor: 5.45 · DOI: 10.1021/jm400715h · Source: PubMed

7 AUTHORS, INCLUDING:

Dorota Gryko
Polish Academy of Sciences
75 PUBLICATIONS **983** CITATIONS
SEE PROFILE

Mikołaj Chromiński
Polish Academy of Sciences
11 PUBLICATIONS **34** CITATIONS
SEE PROFILE

Iraida Sharina
University of Texas Medical School
40 PUBLICATIONS **605** CITATIONS
SEE PROFILE

Emil Martin
University of Texas Medical School
62 PUBLICATIONS **2,639** CITATIONS
SEE PROFILE

Journal of Medicinal Chemistry

Article

pubs.acs.org/jmc

Synthesis and Evaluation of Bifunctional sGC Regulators: Optimization of a Connecting Linker

Mikołaj Chromiński,[†] Łukasz Banach,[†] Maksymilian Karczewski,[†] Keith ó Proinsias,[†] Iraida Sharina,[‡] Dorota Gryko,*[,†] and Emil Martin*[,‡]

[†]Institute of Organic Chemistry, Polish Academy of Sciences, Kasprzaka 44/52, 01-224 Warsaw, Poland

[‡]Department of Internal Medicine, Division of Cardiology, University of Texas Health Science Center in Houston, The University of Texas, 1941 East Road, Houston, Texas 77054, United States

Supporting Information

ABSTRACT: Hybrid molecules composed of PpIX and cobyrinic acid derivatives conjugated through linkers of varying length and composition were prepared via 1,3-dipolar cycloaddition (CuAAC) or amidation/esterification reactions. They were tested for activation of soluble guanylyl cyclase (sGC), a key enzyme in the NO/cGMP signaling pathway, by an in vitro GTP→cGMP conversion assay. Using purified heme-deficient sGC and truncated sGC variants lacking a heme-binding domain, we demonstrate that such hybrid molecules may activate sGC by targeting heme-binding and/or catalytic domain. While all conjugates activated sGC, only selected compounds served as bifunctional regulators and were capable of simultaneous targeting both heme and catalytic domains of sGC. The length and type of a linker connecting both components had a profound effect on the extent of sGC activation, indicating that the linker's type is crucial for their binding affinities with regulatory and catalytic domains. Only hybrids with the conjugated linker of 13−16 atom length synergistically target both domains and displayed the lowest EC_{50} and highest activating potency. Compounds with shorter connecting linkers were much less potent and were no more active than the cobyrinic acid component alone The most active conjugate, which showed a 60-fold activation of sGC, was compound **11**, in which PpIX and cobyrinic acid components are separated by 11 atoms chain with the triazole moiety in between.

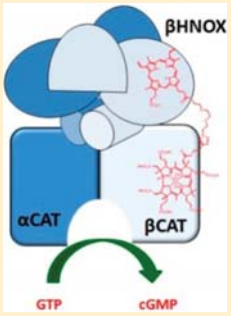

INTRODUCTION

Soluble guanylyl cyclase (sGC) is the principal intracellular receptor for nitric oxide (NO). In response to NO binding to the sGC heme group, the conversion of guanosine triphosphate (GTP) into cyclic guanosine-3′,5′monophosphate (cGMP) is enhanced several hundred fold. sGC is a heterodimeric protein composed of α- and β-subunits.[1] Although two isoforms for each subunit have been identified (α1, α2 and β1, β2), only heterodimers containing the β1 subunit are catalytically active and responsive to the NO stimulus.[2] The $\alpha1\beta1$ heterodimer is the predominant sGC enzyme with almost ubiquitously expression. While the X-ray structure of full-length sGC is not yet available, structure−activity studies clearly identify three independent domains: regulatory, catalytic, and dimerization region, with specific functions integrated into the heterodimer.[3] C-Terminal regions of each subunits form the catalytic domain and both subunits are essential for cGMP synthesis (Figure 1, CAT domains). Furthermore, the interaction between central domains of α- and β-subunits contributes to the formation of a stable heterodimer (CC and PAS domains) and mediation of stimulatory signal induced in the N-terminal regulatory domain (PAS and HNOX domains). N-Terminal regions of both subunits are critical for sGC activation because the N-terminal part of the β subunit harbors the heme moiety (βHNOX), while the N-terminal α subunit is involved in the interaction with allosteric stimulators of sGC (αHNOX).

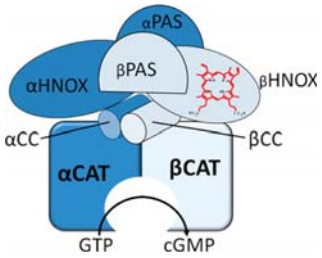

Figure 1. Schematic representation of sGC architecture. Shown is the hypothetical orientation of domains in $\alpha1\beta1$ sGC heterodimer based on previous studies.[4,5] αCAT and βCAT, guanylyl cyclase catalytic domains; αCC and βCC, coil−coil elements; αPAS and βPAS, PAS-like regions; βHNOX, heme-NO/oxygen binding domain of the β subunit; αHNOX, amino-terminal domain of the α subunit.

Under proper physiological conditions, binding of NO to the heme moiety induces a set of transformations leading to enhanced cGMP synthesis. Thus, activated sGC is a key component in the NO/cGMP signaling that governs various physiological processes. These include, but are not limited to, vascular smooth muscle relaxation, electrolyte homeostasis, platelet function, neurotransmission, mitochondrial neogenesis, etc.[6] Many pathological conditions lead to impaired bio-

Received: May 14, 2013

   dx.doi.org/10.1021/jm400715h | J. Med. Chem. XXXX, XXX, XXX−XXX

Chart 1. Structure of sGC Activators

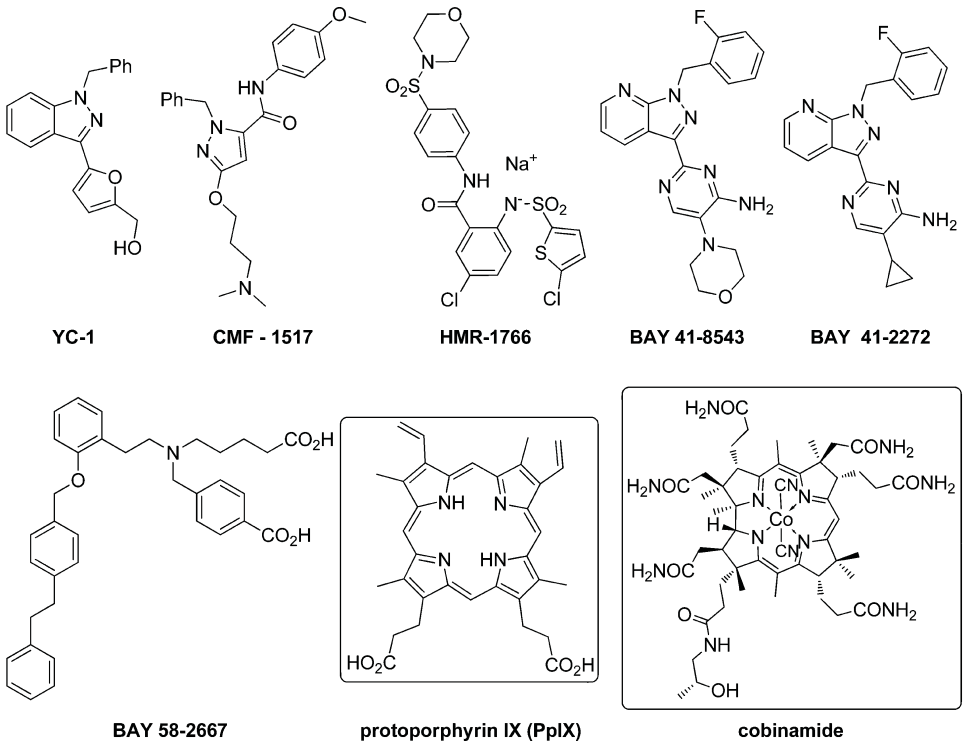

availabilty of endogenous NO, which leads to cardiovascular and other diseases.[7] Supplementation of NO in various forms of organic nitrates is currently the most widely used approach to benefit from pharmacological upregulation of sGC activity. However, this strategy has a number of limitations: decreased efficacy over time due to the development of tolerance to organic nitrates, formation of reactive nitrogen species which damages proteins, DNA, and lipids, etc.[8] As an alternative, an increasing number of NO-independent regulators of sGC has been identified, including protoporhyrin IX (PpIX), YC-1, BAY 41-2272, BAY 41-8543, BAY 58-2667, HMR-1766, and CMF-1571 (Chart 1).[9] Despite their structural diversity and different mechanism of action, all these compounds target the regulatory domain.

On the contrary, we have recently demonstrated that cobinamide and cobyrinic acid derivatives activate sGC via targeting the catalytic domain.[10,11] Our studies indicated that cobinamide synergistically potentiate the effect of NO-independent sGC upregulators, such as BAY41-2272 and YC-1, BAY58-2667, and HMR1766.

This unique mode of action opened the possibility to design sGC regulators that can act simultaneously on regulatory and catalytic domains. Hence, we have found that conjugates composed of protoporphyrin IX and cobyrinic acid derivatives have up to 30-fold higher potency than both components independently.[12] These studies also suggested that the length of a linker connecting both components plays a crucial role in determining the efficiency of sGC activation. However, the optimal length and type of a linker that induce the most effective activation of sGC has not been determined yet. Herein, we present structure–activity relationship (SAR) studies showing the contribution of linker features to sGC activation. Toward this end, a series of hybrid molecules with various linkers and linkages were prepared and their effect on sGC was tested.

RESULTS AND DISCUSSION

Chemistry. In this approach, the connected components, hexamethyl cobyrinate and PpIX derivatives, targeting, respectively, catalytic and regulatory domains, remained unchanged. The synthesis of such hybrids involved selective preparation of cobyrinate and PpIX building blocks possessing suitable terminal functional groups, e.g., –alkyn, $-N_3$, $-NH_2$, and –OH. Subsequently, copper catalyzed azide–alkyne 1,3-dipolar cycloaddition reaction (CuAAC)[13] or amidation/esterification reactions were utilized to connect both activators.[14,15]

Cobyrinic acid derived building blocks **3a–i** were prepared starting from *c*-acid **1** via esterification and amidation reactions (Scheme 1). Although it was previously suggested that the aqua complex of *c*-acid **1** is more reactive toward these types of modifications,[15] we found that dicyano form worked equally well. Thus, $(CN)_2Cby(OMe)_6$(*c*-acid) **1** was reacted with a series of "clickable" derivatives **2a–e** in the presence of EDC/DMAP, generating desired building blocks **3a–e** in high yields.[12] For reactions of *c*-acid **1** with aminoalcohol **2f** and diamines **2g–i**, DEPC turned out to be a superior coupling reagent.[15]

Functionalization of PpIX with proper linkers was performed in a similar manner by EDC/DMAP mediated esterification or amidation reactions. Though, our previously described methodology for the synthesis of "clickable" PpIX derivatives was effective, we encountered some solubility issues.[12] To circumvent this problem, one of PpIX carboxylic groups was protected with 2-(trimethylsilyl)ethanol, giving monoester **4** as a mixture of two regioisomers in 68% yield (Scheme 2).[16] It was then reacted with various alcohols **2a,j,e,k** and amine **2l** in the presence of EDC, providing desired products **5a–e** in excellent yields.

dx.doi.org/10.1021/jm400715h | J. Med. Chem. XXXX, XXX, XXX–XXX

Scheme 1. Synthesis of Cobyrinic Acid Derived Building Blocks

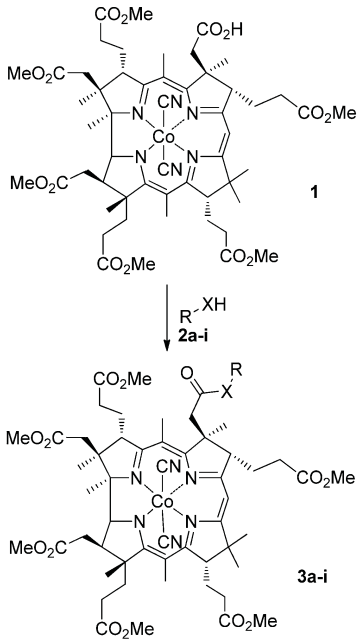

substrate 2	R-X	product 3	yield (%)
2a		**3a**	91
2b	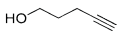	**3b**	89
2c		**3c**	85
2d		**3d**	75
2e	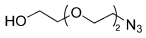	**3e**	89
2f	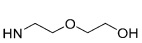	**3f**	76
2g	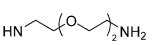	**3g**	65
2h	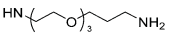	**3h**	54
2i	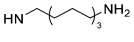	**3i**	58

Scheme 2. Synthesis of PpIX Building Blocks

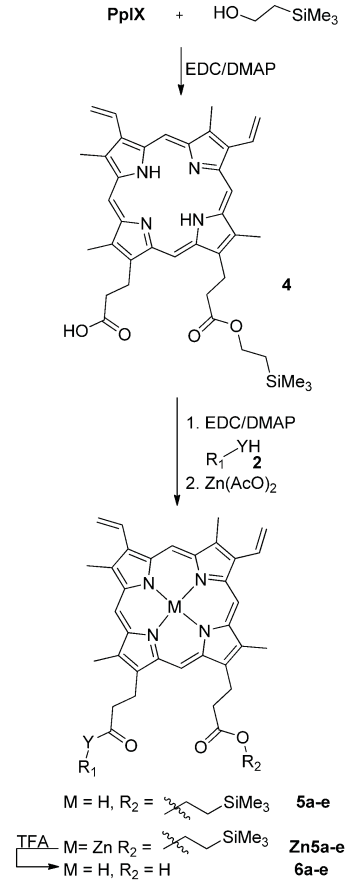

RYH	YR	product	yield (%)
2j	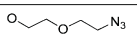	**Zn5a**	96
2e	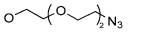	**Zn5b**	85
2k	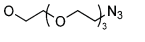	**Zn5c**	90
2l	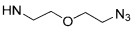	**Zn5d**	95
2a	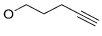	**Zn5e**	98

Introduction of the nonpolar TMS group assured not only good solubility in organic solvents facilitating purification of building blocks **5a−e** but also improved stability of their Zn complexes **Zn5a−e**.

Subsequently, synthesized Cby and PpIX derivatives, respectively **3** and **Zn5**, were reacted in a two-step process involving the CuOAc-catalyzed alkyne−azide cycloaddition[13b] followed by treatment with TFA in DCM both to remove the protecting group and to demetallate the PpIX macrocyclic core (Scheme 3).[12,16] Although the one-pot procedure, reported previously, requires one purification step less,[12] we found it more convenient to separate these two steps with a simple workup and gel filtration.

Using the improved synthetic methodology, a library of hybrid molecules **7−22** was synthesized. Depending on the linker attached, yields for CuAAC/deprotection sequence varied from moderate to very good. Unexpectedly, all hybrids **15−18** derived from *c*-propargyl amide **3c** appeared to be highly unstable. Other molecules in the series were stable and could be stored even for months without decomposition.

To further investigate how the nature of the linker affects sGC activation, we designed a hybrid molecule with reversed linker composition. Using conjugate **12**, in which both activators are separated by 14-atom chain, as a reference, hybrid analogues were prepared. The reaction of azide **3e** with

dx.doi.org/10.1021/jm400715h | J. Med. Chem. XXXX, XXX, XXX−XXX

Scheme 3. Synthesis of PpIX−Corrin Hybrids 7−22 via CuAAC

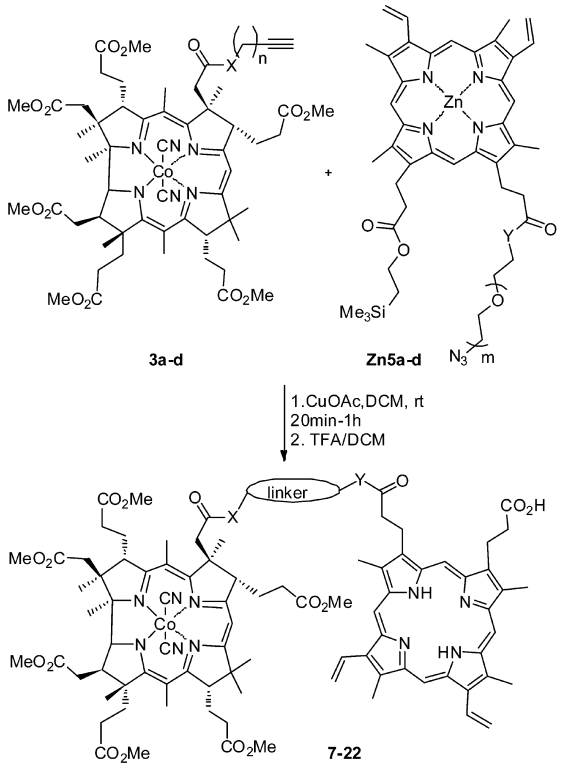

linker[a]	product	yield (%)	linker[a]	product	yield (%)
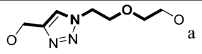	**7**	70	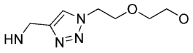	**15**	0[b]
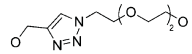	**8**	58	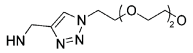	**16**	0[b]
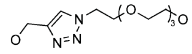	**9**	61	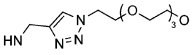	**17**	0[b]
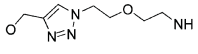	**10**	27	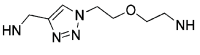	**18**	0[b]
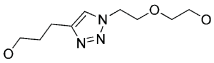	**11**	47	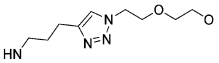	**19**	70
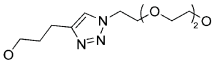	**12**	86	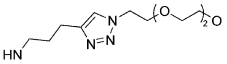	**20**	56
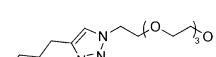	**13**	41	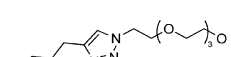	**21**	39
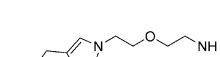	**14**	60	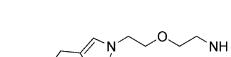	**22**	79

[a]As a length of the linker a number of atoms starting from the first carbon on the Cby site finishing on the last carbon on the PpIX site was adopted. The triazole unit was counted as 2 atoms

[b]Hybrids were unstable.

alkyne **Zn5e** under standard CuAAC/deprotection conditions furnished compound **23** in 73% (Scheme 4).

Furthermore, we evaluated the contribution of the triazole moiety on the extent of sGC activation by synthesizing a series

dx.doi.org/10.1021/jm400715h | J. Med. Chem. XXXX, XXX, XXX−XXX

Scheme 4. The Synthesis of Hybrid 23

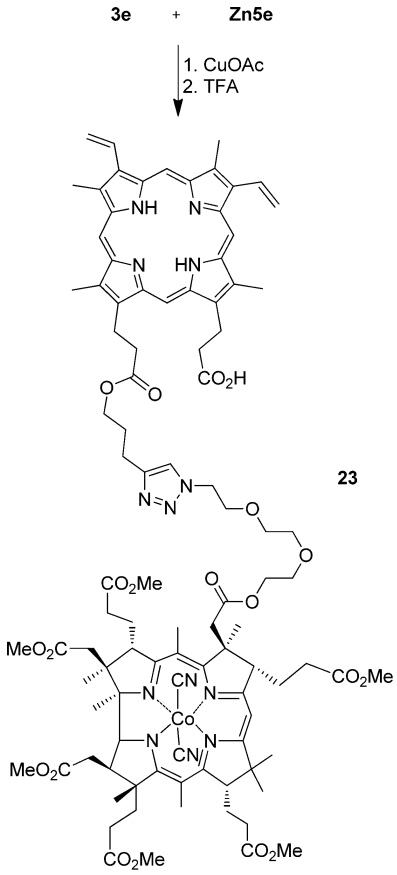

of hybrids with linkers devoid of this unit. Again, mono (2-trimethylsilyl)ethyl ester **4** proved to be a valuable starting material, as the use of unprotected PpIX in reactions with amines led predominantly to the formation of diamides. Hence, when ester **4** was reacted with $(CN)_2$Cby derivatives **3f–i**, desired hybrids **24a–d** were obtained as a mixture of regioisomers in moderate to good yields (Scheme 5). Subsequent treatment with TFA afforded hybrids **25a–d** possessing free carboxylic group.

An alternative position of a linker attachment was also considered. A hybrid molecule in which the linker was anchored by the amide linkage to the *meso* position of heptamethyl cobyrinate was designed. A known $(CN)_2$Cby derivative bearing an amine functionality at the 10 position was coupled with pent-4-ynoic acid, in accordance with a literature procedure, giving alkyne **26** in 87% yield.[17,18] Subsequently, using our standard CuAAC/deprotection sequence, hybrid **27** was isolated in 64% yield (Scheme 6).

For all new compounds described above, their effect on sGC was tested.

Biology. *Maximal Activation by Hybrids Requires Both Domains.* As a first step in our studies, we validated our premise that corrin–PpIX hybrids may act as dual ligand activators, which target both the heme-binding region and the catalytic domain.

First, we tested how the presence of sGC heme influenced the enzyme activation by corrin–PpIX hybrids. For this purpose, a previously established procedure[20] was used to deplete sGC heme by incubating the enzyme with low concentration of Tween 20. Early studies demonstrated that such treatment facilitate the incorporation of PpIX in the heme binding pocket and leads to stronger activation by PpIX.[21,22] As demonstrated in Figure 2A, the heme depletion resulted in a leftward shift of the dose–response curves for corrin–PpIX hybrids **11** and **12**, and a lower EC_{50} (31 vs 5.4 μM for **11** and 72 vs 25 μM for **12**, Table 1, entries 5, 6), arguing for improved affinity. A similar trend was observed for all tested hybrids (data not shown). In some cases, e.g., **12**, increased maximal sGC activation was also observed (Figure 2A). This improved affinity and activation potency of new hybrids could be attributed primarily to the activation by the porphyrin moiety of a molecule because only PpIX building block **6b** was affected by heme depletion (Figure 2B), while the corrin building block **3b** was not (Figure 2C).

Next, we confirmed that the cobyrinic acid moiety of hybrid molecules targets the catalytic region of the enzyme. For this purpose, we compared the effect of hybrid molecules, porphyrin and cobyrinic acid components on two sGC enzymes, full-length $\alpha1\beta1$ sGC and the truncated $\alpha1$CAT/$\beta1$CAT enzyme, which lacks N-terminal regulatory regions, including the heme-binding domain (Figure 2E). As expected from previous studies,[11,12] $(CN)_2$Cbi, both corrin and porphyrin building blocks **3b** and **6b**, respectively, activated the full length sGC (Figure 1D). Corroborating our previous observations, tested hybrid molecules **11** and **12** showed stronger activation of $\alpha1\beta1$ sGC than any of the constituting building blocks **3b** and **6b** (Figure 2D, light bars). However, when the response to these compounds was tested on the $\alpha1$CAT/$\beta1$CAT mutant (Figure 1D, black bars), the porphyrin building block **6b** had no effect on activity while the activation by the hybrid molecules was significantly reduced. Consistent with the premise that cobyrinates target the catalytic region of sGC, $(CN)_2$Cbi, cobyrinate **3b**, and the hybrid molecules activated sGC to a similar extent. In combination, the data presented in Figure 2 supports our hypothesis that the porphyrin moiety of the hybrid molecule requires the heme region for sGC activation, while the cobyrinate moiety targets the catalytic domain. Thus, these hybrids can be regarded as designed multiple ligands (DML). The term, coined by Morphy, describes compounds acting on multiple targets and whose multiple biological profiles are rationally designed to address a particular dysfunction, with the overall goal of enhancing efficacy and/or improving safety.[19] Other proposed names include hybrid molecules, heterodimer, dual ligands, etc. Our conjugates belong to DMLs group composed of pharmacophore elements for each target which are well separated by a linker. Because all hybrid molecules described in this work contain two active pharmacophore groups well separated by a linker, they can be regarded as dual ligand conjugates even though they act on one target.

Determining the Optimal Linker Length and Composition. Having confirmed that both porphyrin and cobinamide moieties of the hybrid contribute to sGC activation, we investigated how the length and composition of different linkers affect sGC activation. To determine the optimal length of the linker, we compared the dose–response sGC activation curves for compounds **7–9** and **11–13**, which carry the ester-conjugated linkers of a 9–17-atom chain. As shown in Figure 3A, the extent of sGC activation varied depending on the length of a linker. While all tested conjugates **7–9** and **11–13** activated sGC, hybrids **11**, **8**, and **12** with 11, 12, and 14 atoms linkers, respectively, were the most effective sGC activators. These molecules displayed the strongest maximal activation

dx.doi.org/10.1021/jm400715h | J. Med. Chem. XXXX, XXX, XXX–XXX

Scheme 5. Synthesis of PpIX−Corrin Gybrids 25a−d via Amidation/Esterification Reaction

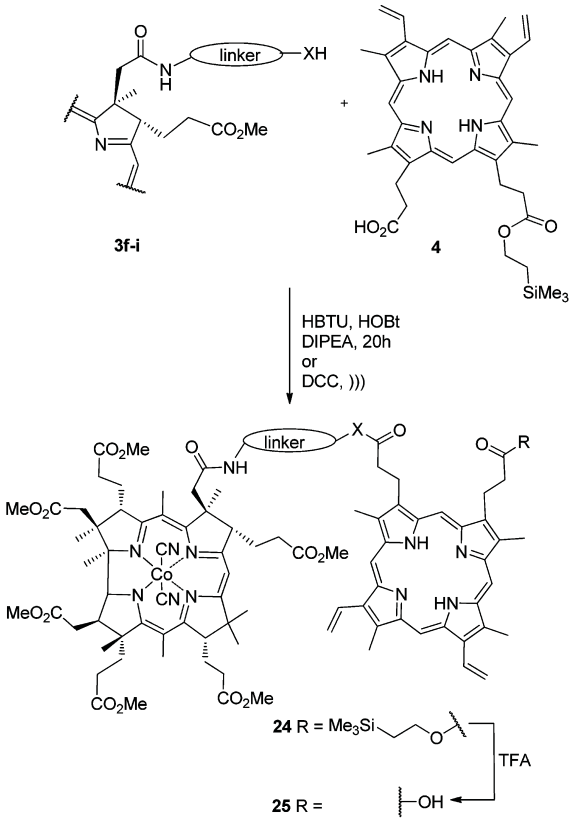

linker	R	product	yield (%)
	OCH_2CH_2TMS	**24a**	35
	OH	**25a**	73
	OCH_2CH_2TMS	**24b**	61
	OH	**25b**	73
	OCH_2CH_2TMS	**24c**	64
	OH	**25c**	74
	OCH_2CH_2TMS	**24d**	59
	OH	**25d**	71

(Figure 3B) and the smallest EC_{50} (Figure 3C, Table 1, entries 2, 5, and 6) among all tested.

A working structural model of the sGC heme domain was previously derived from the X-ray structure of the HNOX homologue from cyanobacteria[23] and later experimentally validated.[24,25] As shown in Figure 3D, this model predicts that the access to one of heme's propionic groups is blocked by several residues (Figure 3D, yellow propionate). However, the second propionic group (Figure 3D, pink propionate) points directly to a narrow opening in the heme domain, through which the conjugating linker may lead away. In addition to structural model of the heme domain, the X-ray structure of the sGC catalytic domain has been reported recently.[26] In spite of these advancements in our understanding of sGC structure, currently there is no clear picture of the architecture of the full-length sGC protein and of the orientation of heme and catalytic domains with respect to each other. Because the maximal activation of sGC is expected when both corrin and porphyrin

dx.doi.org/10.1021/jm400715h | J. Med. Chem. XXXX, XXX, XXX−XXX

Scheme 6. The Synthesis of Hybrid 27

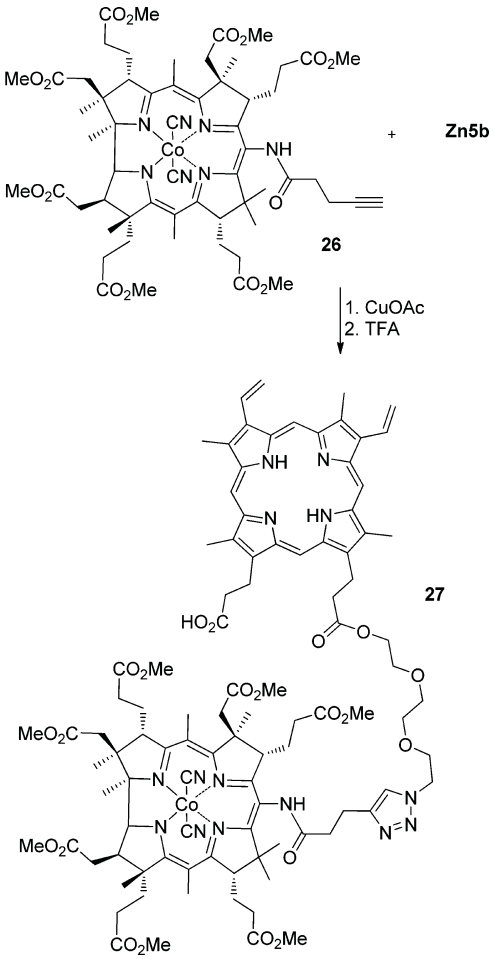

moieties are bound to their corresponding binding sites, the data in Figure 3 suggest that these sites are relatively close to each other and are separated by a distance that spans 11−14 atom bonds. This indicates that the catalytic domain and the heme domain are in close proximity to each other.

In addition to the linker length, the position of the triazole group within the context of the linker also appears to contribute to the effectiveness of the hybrid as sGC activator. Although both compounds **23** and **12** contain linkers of the same length and composition, but reverse orientation, DML **12** was more effective than DML **23**. Inspection of the structural model of the sGC heme domain suggests that, depending on the linker orientation, the bulkier triazole group within the putative escape channel (Figure 3D) may clash with the Tyr2, Asp44, Arg116, or Ile142 residues lining this channel. Such steric constrains may explain the observed difference between compounds **12** and **23**).

We next investigated whether changing the ester linkage with the amide affects the extent of sGC activation. We tested several hybrids **19**−**21** with amide conjugated linkers of 11-, 14-, and 17-atom length. We found that conjugates with amide linkages were less effective than those possessing ester linkage of the same length (Figures 3A and 4A). In fact, **20**, the most potent compound of this type, was no more potent than the corrin component alone. This suggests that sGC activation by this type of hybrids is primarily due to the function of the corrin moiety. In the case of compounds **10**, **14**, and **19**−**22**, there is a possibility that the amide groups forms a hydrogen bond with the nearby triazole moiety, locking the linker in a conformation that restricts the binding of both activating groups of the hybrid. Interestingly, compound **21**, carrying the longest linker composed of 17 atoms, displayed a bell-shaped activation curve. This behavior is consistent with our previous studies of sGC activation by cobinamide derivatives.[10,27] These studies suggested the existence of two cobinamide-binding sites: a high affinity activating site and a low affinity inhibitory site.

We also tested if linkers lacking the triazole group offer any advantage. As demonstrated in Figure 4B, corrin−PpIX hybrids **25a**−**d** conjugated with linkers lacking the triazole group were less effective sGC activators. Compound **25a**, the most potent of this type, was only as effective as the cobyrinate component **3b** alone. It is clear that the hybrid with a flexible linker may take a great number of conformations, not all of them optimal for the binding of cobyrinate and PpIX derivatives to their biding sites. It is possible that the triazole moiety diminishes the flexibility of the linker or provides additional interactions with sGC residues, thus facilitating the bifunctional activation. Future studies will indicate whether the introduction of a more rigid linker or placement of triazole in different positions along the linker will change the potency of the hybrid.

Finally, we evaluated whether the position of a linker anchoring to the cobyrinic acid moiety is important for the potency of sGC activation. As demonstrated in Figure 5, the conjugate with the linker anchored to the 10 position of the cobyrinic acid was less potent than the conjugate with similar linker attached at 7 position. The difference in the activation potency is most probably due to some steric constraints that hinder the proper binding of the cobyrinate group to the catalytic domain when the linker is in position 10. Only when structure−function studies of sGC will identify the allosteric site to which cobinamide binds can the the exact nature of these steric constraints be determined in the future.

CONCLUSION

We have designed a set of novel bifunctional regulators, possessing of both corrinoid and PpIX units, of soluble guanylyl cyclase. Protoporphyrin IX derivatives, which targets the sGC heme domain, are conjugated with cobyrinic acid derivatives, which was demonstrated to target the sGC catalytic region. A series of such conjugated DMLs with various linkers and linkages was synthesized using optimized procedures for the CuOAc-catalyzed 1,3-dipolar cycloaddition reaction or amidation/esterification reactions. All DMLs prepared are stable compounds except those derived from propargyl amide **3c**, suggesting that their stability strongly depends on the type of the linkage. The length and composition of the linker was proved to be crucial for potent sGC activation. Our results indicate that only hybrid molecules containing the conjugating linker of 13−16-atom chain benefited from synergistic engagement of both regulatory heme-binding region and catalytic domain. The most effective compound, **11**, contained an 11-atom chain linker with the triazole group positioned close to the corrin moiety. This compound displayed more than 60-fold activation of sGC. Hybrids with shorter linkers, or with different linker composition, were much less potent and were no more active than the cobyrinic acid component alone. These studies reinforce the concept that cobinamides can be used as costimulators of sGC activity and in vivo function and demonstrate the proof of principle for multiple ligand sGC regulators. Structural insights obtained from these studies lay

dx.doi.org/10.1021/jm400715h | J. Med. Chem. XXXX, XXX, XXX−XXX

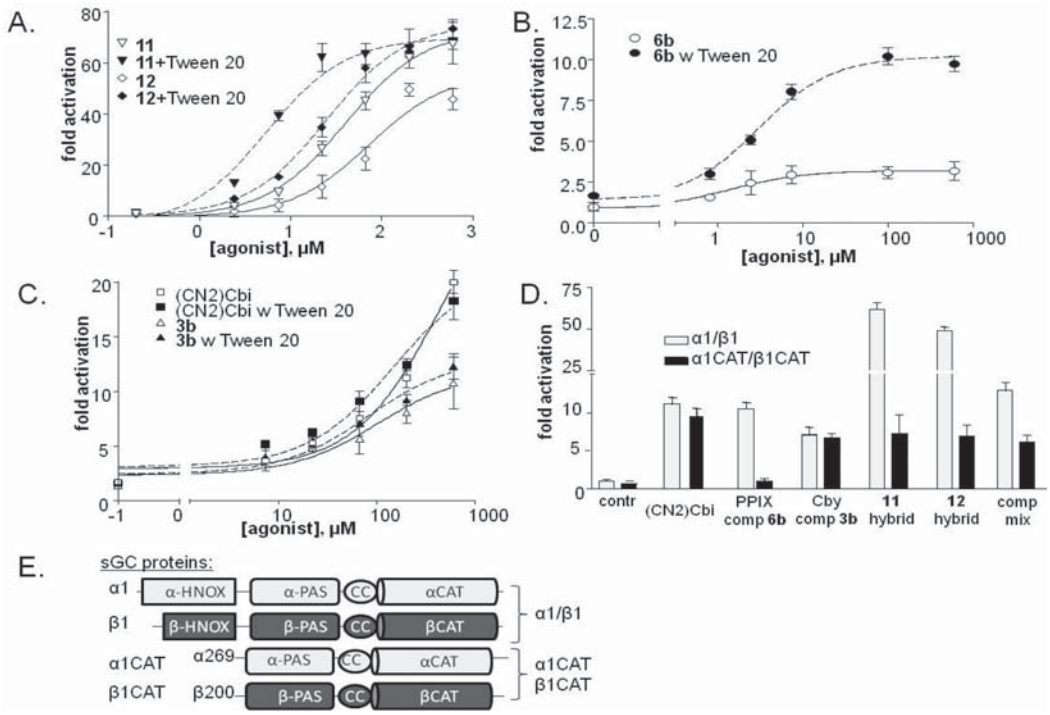

Figure 2. Cobyrinic acid−PpIX conjugates are bifunctional sGC activators. Depletion of sGC heme enhances the activation by corrin−PpIX conjugates (A) and its PpIX component (B), but not the cobyrinate moiety (C). For (A−C), data are shown as fold activation (mean ± SD) over basal sGC activity (73 ± 5 nmol/min/mg). (D) cGMP-forming activity was tested for full-length ($\alpha1\beta1$) and truncated sGC ($\alpha1CAT\beta1CAT$) enzymes in the presence of 200 μM protoporphyrin component (PpIX comp), cobyrinate component (Cby comp), and their stoichiometric mixture (comp mix). Activation by 200 μM of hybrid molecules **11**, **12**, and dicyanocobinamide ($(CN)_2Cbi$) is also shown. Data are presented as fold activation (mean ± SD) over basal activity. Basal activity for $\alpha1\beta1$ was 73 ± 5 nmol/min/mg, while for $\alpha1CAT\beta1CAT$ it was 31 ± 4 nmol/min/mg. (E) Schematic representation of the domain structure of the wild-type $\alpha1\beta1$ and the truncated $\alpha1CAT\beta1CAT$ sGC. The position of the first residue of the $\alpha1CAT$ and $\beta1CAT$ is shown with respect to the numeration of the corresponding full-length subunits.

the foundation for creation of future bifunctional sGC regulators containing corrin derivatives. The library of generated cobyrinic acid building blocks created for "click chemistry" can be used for generation of more potent hybrids, e.g., hybrids with other heme-targeting sGC regulators.

EXPERIMENTAL SECTION

Chemistry. *General and Materials.* All solvents and chemicals used in syntheses were of reagent grade and were used without further purification. Tested compounds had >95% chemical purity as measured by elemental analysis. Unless otherwise stated, all NMR spectra were recorded at room temperature. Vitamin B_{12} was purchased from Aldrich.

Synthesis of $(CN)_2Cby[(OMe)_6$-*c*-propargyl ester] **3a** and $(CN)_2Cby[(OMe)_6$-*c*-pent-4-yn ester] **3d** was previously described.[12] Procedure developed for the synthesis of **3a** was subsequently used for the synthesis of compounds **3c−e**. DMLs **7**,[12] **11**,[12] and **12**[12] were previously described, while DMLs **15−18** were unstable and decomposed during chromatographic purification. The synthesis of compound **26** was previously described.[18]

*$(CN)_2Cby[(OMe)_6$-c-propargyl Amide] (**3c**).* Starting from acid **1** (150 mg, 0.140 mmol), compound **3c** was isolated as a purple solid (120 mg, 85% yield). R_f 0.4 (5% MeOH in DCM). Anal. Calcd for $C_{56}H_{74}CoN_7O_{13} + H_2O$: C 59.51, H 6.78, N 8.68. Found: C 59.77, H 6.53, N 8.51. MS ESI (*m*/*z*): calcd for $C_{55}H_{74}CoN_6O_{13}$ $[M - CN]^+$ 1085.46, found 1085.40; for $C_{56}H_{74}CoN_7O_{13}Na$ $[M + Na]^+$ 1034.46, found 1034.40. UV/vis CH_2Cl_2, λ_{max} (nm) (ε, $L{\cdot}m^{-1}{\cdot}cm^{-1}$): 589 ($1.09 \times 10^4$), 550 ($8.60 \times 10^3$), 422 ($2.85 \times 10^3$), 371 ($2.92 \times 10^4$), 317 ($9.25 \times 10^3$), 279 ($1.23 \times 10^4$). ^1H NMR (500 MHz, $CDCl_3$) δ (ppm): 7.47 (t, *J* = 5.5 Hz, 1H), 5.54 (s, 1H), 3.89 (ddd, *J* = 17.3, 5.5, and 2.4 Hz, 2H), 3.80−3.72 (m, 2H), 3.77 (s, 3H), 3.71 (s, 3H), 3.70 (s, 3H), 3.69 (s, 3H), 3.68 (s, 3H), 3.64 (s, 3H), 3.05 (dd, *J* = 6.7 and 4.4 Hz, 1H), 2.86−2.79 (m, 1H), 2.68−2.59 (m, 4H), 2.58−2.35 (m, 8H), 2.34−2.26 (m, 3H), 2.24 (s, 3H), 2.23−2.14 (m, 4H), 2.13 (s, 3H), 2.08 (t, *J* = 2.4 Hz, 1H), 2.10−1.95 (m, 2H), 1.87−1.74 (m, 2H), 1.79 (s, 3H), 1.74−1.59 (m, 3H), 1.51 (s, 3H), 1.36 (s, 3H), 1.28 (s, 3H), 1.21 (s, 3H). ^{13}C NMR (125 MHz, $CDCl_3$) δ (ppm): 175.8, 175.7, 175.4, 173.8, 173.6, 172.8, 172.6, 171.7, 171.6, 171.1, 169.4, 163.5, 160.6, 135.9, 129.1, 107.0, 102.2, 91.4, 82.7, 79.9, 74.7, 70.4, 58.9, 58.4, 57.0, 53.5, 52.4, 51.83, 51.79, 51.61, 51.58, 51.5, 47.1, 46.9, 45.7, 41.3, 39.2, 33.6, 32.4, 31.7, 31.5, 30.9, 30.7, 29.6, 28.7, 25.7, 25.6, 24.8, 22.1, 19.7, 19.3, 18.4, 16.9, 15.7, 15.2.

*$(CN)_2Cby[(OMe)_6$-c-pent-4-yn Amide] (**3d**).* Starting from acid **1** (150 mg, 0.140 mmol), compound **3d** was isolated as a purple solid (119 mg, 75% yield). R_f 0.4 (5% MeOH in DCM). Anal. Calcd for $C_{58}H_{78}CoN_7O_{13} + H_2O$: C 60.15, H 6.96, N 8.47. Found: C 60.23, H 7.09, N 8.49. MS ESI (*m*/*z*) calcd for $C_{57}H_{78}CoN_6O_{13}$ $[M - CN]^+$ 1113.50, found 1113.50; for $C_{58}H_{78}CoN_7O_{13}Na$ $[M + Na]^+$ 1162.49, found 1162.50. UV/vis (CH_2Cl_2), λ_{max} (nm) (ε, $L{\cdot}m^{-1}{\cdot}cm^{-1}$): 589 ($1.15 \times 10^4$), 550 ($8.57 \times 10^3$), 423 ($2.85 \times 10^3$), 371 ($2.89 \times 10^4$), 317 ($9.30 \times 10^3$), 279 ($1.24 \times 10^4$). ^1H NMR (500 MHz, $CDCl_3$) δ (ppm): 7.09 (t, *J* = 5.5 Hz, 1H), 5.55 (s, 1H), 3.77 (s, 3H), 3.71 (s, 6H), 3.70 (s, 3H), 3.68 (s, 3H), 3.64 (s, 3H), 3.48−3.37 (m, 1H), 3.08−3.02 (m, 1H), 2.97−2.88 (m, 1H), 2.86−2.78 (m, 1H), 2.67 (dd, *J* = 9.4 and 4.5 Hz, 1H), 2.64−2.34 (m, 10H), 2.33−2.26 (m, 2H), 2.24 (s, 3H), 2.22−2.12 (m, 4H), 2.10 (s, 3H), 2.08−1.96 (m, 2H), 1.90 (s, 1H), 1.88 (t, *J* = 2.6 Hz, 1H), 1.86−1.81 (m, 2H), 1.79 (s, 3H), 1.77−1.55 (m, 6H), 1.51 (s, 3H), 1.38 (s, 3H), 1.37 (s, 3H), 1.27 (s, 3H), 1.21 (s, 3H). ^{13}C NMR (125 MHz, $CDCl_3$) δ (ppm): 175.9, 175.7, 175.3, 173.8, 173.5, 172.8, 172.5, 171.6, 171.4, 171.3, 169.6, 163.5, 161.2, 106.6, 102.2, 91.3, 83.4, 82.6, 74.6, 68.6, 58.7, 58.4, 56.5, 53.5, 52.4, 51.9, 51.80, 51.79, 51.57, 51.55, 51.4, 47.2, 46.9, 46.1, 41.7, 39.2, 38.7, 33.6, 32.4, 31.7, 31.4, 30.8, 30.7, 29.60, 29.58, 27.9, 25.7, 25.6, 24.8, 22.0, 19.7, 19.2, 18.4, 16.9, 16.1, 15.29, 15.27.

dx.doi.org/10.1021/jm400715h | J. Med. Chem. XXXX, XXX, XXX−XXX

Table 1. EC_{50} Values for Conjugates 7−22, 24a−d, and Compound 3b

entry	linker	product	EC50 (μM)	max. fold activation
1	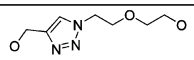	**7**	146	11.0 ± 2.1
2	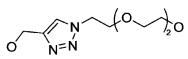	**8**	57	59.0 ± 1.5
3	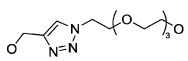	**9**	133	59.0 ± 1.5
4	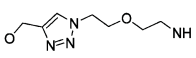	**10**	>400	2.5 ± 0.4
5	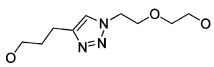	**11**	31	67.4 ± 2.1
6	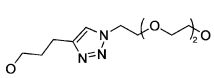	**12**	79	53.7 ± 4.0
7	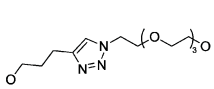	**13**	150	13.0 ± 2.0
8	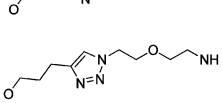	**14**	N/A	1.3 ± 0.1
9	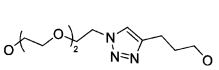	**23**	89	13.2 ± 1.4
10	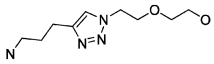	**19**	136	5.3 ± 0.9
11	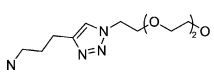	**20**	139	11.7 ± 0.8
12	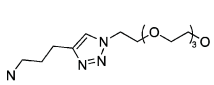	**21**	25	6.1 ± 0.6
13	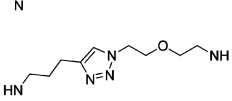	**22**	N/A	0.9 ± 0.2
14	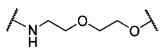	**24a**	30	11.4 ±0.7
15	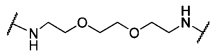	**24b**	6.4	3.7 ± 0.8
16	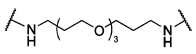	**24c**	N/A	1.9 ±0.1
17	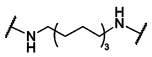	**24d**	N/A	2.2 ± 0.1
18	Cobinamide component	**3b**	79	10.8 ±1.4

*$(CN)_2$Cby[$(OMe)_6$-c-2-(2-[2-azidoetoxy]ethoxy)ethyl Ester] (**3e**).* Starting from acid **1** (75 mg, 0.07 mmol), compound **3e** was isolated as a purple solid (76 mg, 89% yield). R_f 0.5 (5% MeOH in DCM). Anal. Calcd for $C_{59}H_{82}CoN_9O_{16}$ + H_2O: C 56.68, H 6.77, N 10.08. Found: C 56.42, H 6.93, N 9.83. MS ESI (m/z): calcd for $C_{58}H_{82}CoN_8O_{16}$ $[M - CN]^+$ 1205.52, found 1205.52; for $C_{59}H_{82}CoN_9O_{16}Na$ $[M + Na]^+$ 1254.51, found 1254.51. UV/vis (CH_2Cl_2), λ_{max} (nm) (ε, $L{\cdot}m^{-1}{\cdot}cm^{-1}$): 589 ($1.20 \times 10^4$), 552 ($8.45 \times 10^3$), 423 ($2.69 \times 10^3$), 371 ($2.90 \times 10^4$), 317 ($8.38 \times 10^3$), 279 ($1.24 \times 10^4$). ^{1}H NMR (500 MHz, $CDCl_3$) δ (ppm): 5.58 (s, 1H), 4.34 (m, 4H), 3.76 (s, 3H), 3.72 (s, 3H), 3.70 (s, 3H), 3.69 (s, 3H), 3.66 (s, 3H), 3.65 (s, 3H), 3.63 (s, 3H), 3.49−3.44 (m 1H), 3.42−2.34 (m 3H), 3.06−2.98 (m, 2H), 2.87−2.78 (m, 2H), 2.77−2.24 (m, 18H), 2.23 (s, 3H), 2.18 (s, 3H), 2.16−1.98 (m, 2H), 1.89−1.61 (m, 4H), 1.58 (s, 3H), 1.51 (s, 3H), 1.38 (s, 3H), 1.35 (s, 3H), 1.26 (s, 3H), 1.21 (s, 3H). ^{13}C NMR (125 MHz, $CDCl_3$) δ (ppm): 176.2, 175.5, 175.2, 173.9, 173.5, 172.9, 172.7, 171.9, 171.7, 171.4, 170.5, 163.6, 163.4, 103.5, 102.1, 91.2, 82.5, 74.7, 70.6, 70.5, 70.0, 69.0, 63.6, 58.3,

dx.doi.org/10.1021/jm400715h | J. Med. Chem. XXXX, XXX, XXX−XXX

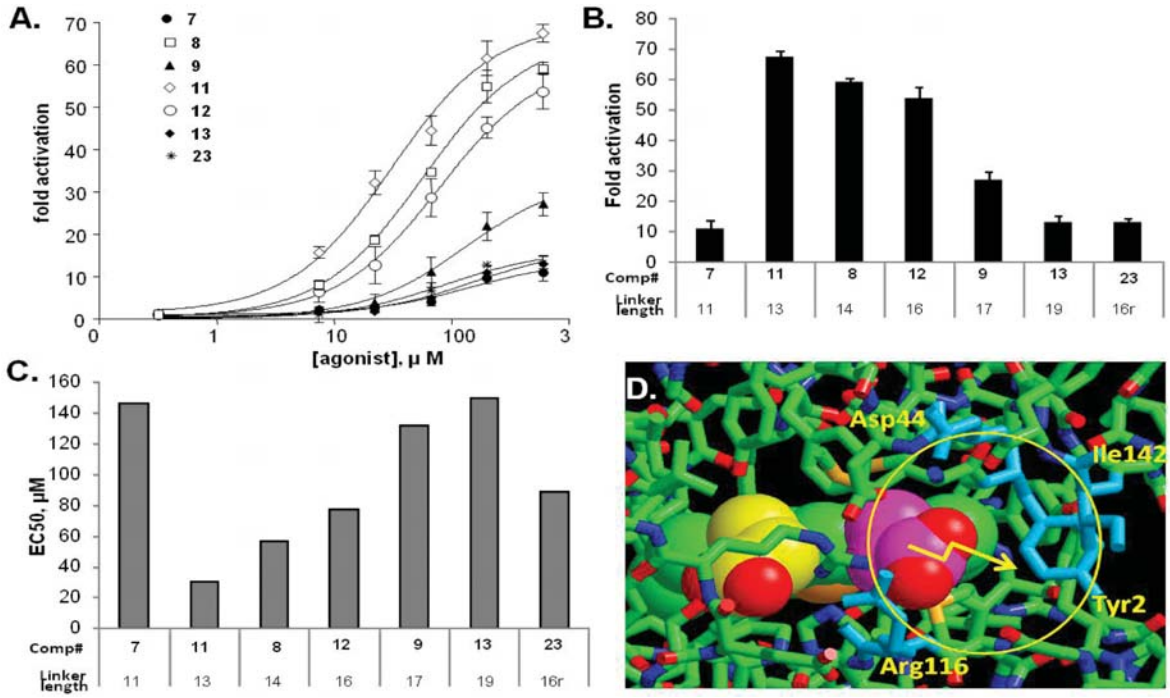

Figure 3. The length of the conjugating linker influences the potency of sGC activation. (A) cGMP-forming activity of $\alpha1\beta1$ sGC in response to different concentrations of cobyrinate−PpIX compounds containing ester-conjugated linkers of varying length. Data are presented as fold activation (mean ± SD) over basal activity (73 ± 5 nmol/min/mg). Both maximal fold activation (B) and the EC_{50} (C) vary depending on the length of the linker. (D) Structural model of the $\beta1$ sGC subunit HNOX heme-binding domain. The heme is shown as a space-fill model with one propionic group in yellow and another in pink. The red spheres are oxygen atoms. Tyr2, Asp44, Arg116, and Ile142 residues lining the putative channel that may fit the conjugating linker are shown in blue. The circle represents the opening of the channel, while the broken arrow represents the conjugating linker.

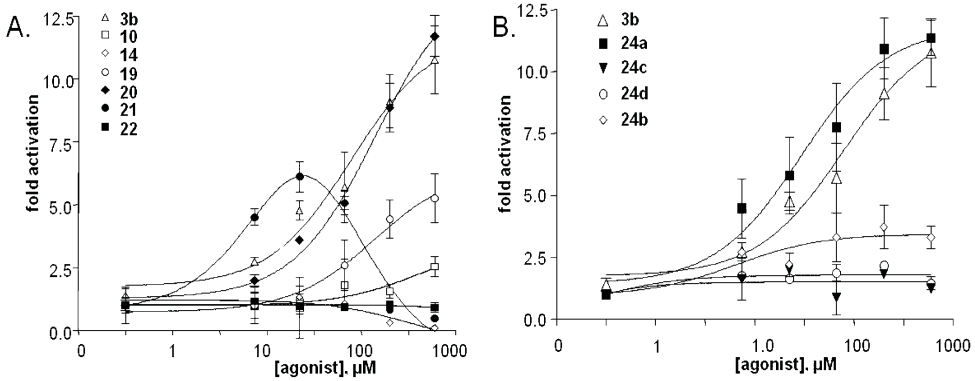

Figure 4. The composition of the conjugating linker influences the potency of sGC activation. (A) cGMP-forming activity of $\alpha1\beta1$ sGC in response to different concentrations of cobyrinate−PpIX compounds containing amide-conjugated linkers of varying length. (B) cGMP-forming activity of $\alpha1\beta1$ sGC in response to different concentrations of cobyrinate−PpIX compounds containing linkers lacking the triazole group. All data are presented as fold activation (mean ± SD) over basal activity (73 ± 5 nmol/min/mg).

56.6, 54.0, 53.6, 52.3, 51.8, 51.7, 51.6, 51.5, 50.6, 48.5, 47.0, 45.5, 42.2, 41.05, 39.2, 33.7, 32.5, 31.8,31.0, 30.7, 29.7, 26.5, 25.7, 24.9, 22.0, 19.8, 19.0, 18.4, 16.9, 15.9, 15.2.

$(CN)_2$Cby[$(OMe)_6$-c-2-(2-hydroxyetoxy)ethylamide] (**3f**). Acid **1** (100 mg, 0.093 mmol) was dissolved in dry DCM (10 mL), and the solution was cooled to 0 °C. DIPEA (50 μL, 0.280 mmol), 2-(2-aminoetoxy)ethanol (33 μL, 0.460 mmol), and DEPC (45 μL, 0.28 mmol) were added. After 30 min, the reaction mixture was allowed to warm to room temperature and then stirred overnight. It was then diluted with DCM (20 mL) and washed with phosphate buffer (pH = 7.2) containing approximately 1% of NaCN. The violet-colored organic phase was then dried over Na_2SO_4, filtered, and concentrated in vacuo. The crude product was purified using DCVC (5% EtOH in DCM). The isolated pure product was redissolved in DCM and washed with phosphate buffer (pH = 7.2) containing approximately 1% of NaCN. The organic phase was dried over Na_2SO_4, filtered, and concentrated in vacuo. Precipitation from AcOEt solution using hexane gave **3f** as violet crystals (82 mg, 76%); mp 92−94 °C. R_f 0.5 (5% MeOH in DCM). Anal. Calcd for $C_{57}H_{80}CoN_7O_{15}$ + $2H_2O$: C 57.13, H 7.07, N 8.18. Found: C 57.25, H 6.76, N 8.0. HRMS ESI (*m*/*z*) calcd for $C_{57}H_{80}CoN_7O_{15}Na$ $[M + Na]^+$ 1184.4937, found 1184.4958. UV/vis CH_2Cl_2, λ_{max} (nm) (ε, $L{\cdot}m^{-1}{\cdot}cm^{-1}$): 588 (1.27 × 10^4), 548 (9.95 × 10^3), 422 (2.84 × 10^3), 371 (3.27 × 10^4), 317 (1.09 × 10^4), 279 (1.23 × 10^4). ^1H NMR (500 MHz, $CDCl_3$) δ (ppm): 7.29 (m, 1H), 5.52 (s,1H), 3.85 (bd, J = 7.9 Hz, 1H), 3.81 (t, J = 5.9 Hz, 1H), 3.77 (s, 3H), 3.71 (s, 3H), 3.70 (s, 3H), 3.70 (s, 3H),

dx.doi.org/10.1021/jm400715h | J. Med. Chem. XXXX, XXX, XXX−XXX

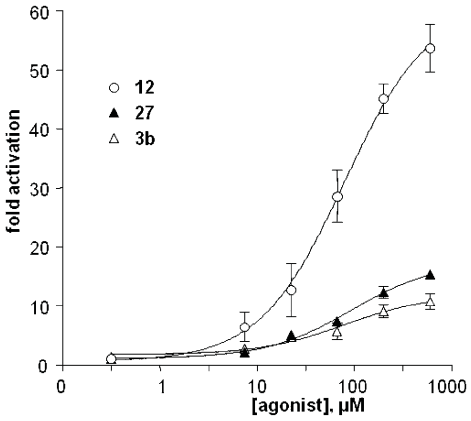

Figure 5. The effect of linker anchoring to the corrin moiety of the conjugate. cGMP-forming activity of $\alpha1\beta1$ sGC in response to corrin−PpIX compounds with the linker attached to position 10 of the corrin macrocycle. Data are fold activation (mean ± SD) over basal activity (73 ± 5 nmol/min/mg).

3.69 (s, 3H), 3.64 (s, 3H), 3.54 (m, 2H), 3.41 (m, 1H), 3.39 (dd, J = 3.2 and 4.5 Hz, 2H), 3.03 (m, 2H), 2.81 (m, 1H), 2.63 (m, 3H), 2.57−2.38 (m, 8H), 2.29 (m, 3H), 2.22 (s, 3H), 2.20−2.12 (m, 4H), 2.10 (s, 3H), 2.08−1.97 (m, 2H), 1.81 (s, 3H), 1.71 (s, 6H), 1.51 (s, 3H), 1.36 (s, 3H), 1.34 (s, 3H), 1.27 (s, 3H), 1.19 (s, 3H). ^{13}C NMR (125 MHz, $CDCl_3$) δ (ppm): 175.9, 175.9, 175.4, 173.8, 173.6, 172.9, 172.5, 172.0, 171.8, 171.0, 169.8, 163.4, 161.1, 106.7, 102.4, 91.2, 82.6, 74.7, 72.6, 69.7, 61.4, 58.7, 58.6, 56.5, 53.5, 52.4, 51.9, 51.8, 51.7, 51.6, 51.4, 47.3, 47.0, 46.1, 41.7, 39.5, 39.2, 33.7, 32.4, 31.7, 31.3, 30.8, 29.7, 25.9, 25.7, 24.8, 22.0, 19.8, 19.2, 18.4, 17.0, 15.31, 15.25.

*$(CN)_2$Cby[$(OMe)_6$-c-2-(2-[2-aminoetoxy]ethoxy)ethylamide] (**3g**).* Following the procedure of **3f**, in which acid **1** (200 mg, 0.19 mmol) was dissolved in dry DCM (20 mL) and DIPEA (100 μL, 0.56 mmol), 3,6-dioxaoctyl-1,8-diamine (135 μL, 0.93 mmol) and DEPC (90 μL, 0.56 mmol) were added. The crude product was purified using DCVC (2−15% MeOH in DCM). Precipitation from the AcOEt solution using hexane gave compound **3g** as violet crystals (145 mg, 65%). R_f 0.3 (11% MeOH in DCM). Anal. Calcd for $C_{59}H_{85}CoN_8O_{15}$ + $3H_2O$: C 56.25, H 7.28, N 8.90. Found: C 56.16, H 7.34, N 8.52. HRMS ESI (m/z): calcd for $C_{58}H_{85}CoN_7O_{15}$ 1178.5430 $[M - CN]^+$, found 1178.5427. UV/vis (CH_2Cl_2) λ_{max} (nm) (ε, L·m^{-1}·cm^{-1}): 588 (8.56×10^3), 551 (8.13×10^3), 422 (2.69×10^3), 371 (2.58×10^4), 312 (8.77×10^3). ^{1}H NMR (500 MHz, $CDCl_3$) δ (ppm): 7.21 (t, J = 5.5 Hz, 1H), 5.57 (s, 1H), 3.77 (s, 3H), 3.71 (s, 3H), 3.70 (s, 6H), 3.67 (s, 3H), 3.63 (s, 3H), 3.54 (bs, 4H), 3.47 (m, 4H), 3.11 (m, 1H), 3.04 (q, J = 3.5 Hz, 1H), 2.95 (dd, J = 4.6 and 8.8 Hz, 1H), 2.81 (t, J = 5.2 Hz, 3H), 2.64−2.59 (m, 3H), 2.58−2.55 (m, 1H), 2.54 (bs, 1H), 2.51−2.47 (m, 2H), 2.46−2.41 (m, 2H), 2.41−2.37 (m, 1H), 2.33 (m, 1H), 2.28 (m, 2H), 2.25 (bs, 1H), 2.23 (s, 3H), 2.20 (m, 1H), 2.17 (m, 1H), 2.15 (m, 1H), 2.12 (s, 3H), 2.08−1.94 (m, 8H), 1.82 (m, 1H), 1.74 (s, 3H), 1.70 (m, 1H), 1.51 (s, 3H), 1.38 (s, 3H), 1.37 (s, 3H), 1.27 (s, 3H), 1.21 (s, 3H). ^{13}C NMR (125 MHz, $CDCl_3$): δ (ppm): 176.0, 175.7, 175.3, 173.9, 173.6, 172.9, 172.6, 171.7, 171.6, 171.6, 169.9, 163.5, 162.2, 105.7, 102.2, 91.3, 82.6, 74.6, 72.8, 70.04, 70.03, 69.3, 58.4, 57.3, 56.7, 53.5, 52.4, 51.9, 51.8, 51.6, 50.7, 46.9, 46.0, 45.9, 41.6, 41.5, 39.2, 39.0, 33.7, 32.4, 31.7, 31.6, 31.3, 30.9, 30.7, 29.6, 26.0, 25.7, 24.9, 22.6, 22.0, 19.8, 19.3, 18.4, 16.9, 15.5, 15.3.

*$(CN)_2$Cby[$(OMe)_6$-c-3-(2-[2-{3-aminopropoxy}ethoxy]ethoxy)-propylamide] (**3h**).* Obtained following the similar procedure as for **3g**, starting from acid **1** (75 mg, 0.07 mmol), compound **3h** was isolated as a purple solid (47 mg, 54% yield). R_f 0.12 (11% MeOH in DCM). Anal. Calcd for $C_{63}H_{93}CoN_8O_{16}$ + $2H_2O$: C 57.61, H 7.44, N 8.53. Found: C 57.66, H 7.31, N 8.33. HRMS ESI (m/z): calcd for $C_{62}H_{93}CoN_7O_{16}$ 1250.6005 $[M - CN]^+$, found 1250.6024. UV/vis (CH_2Cl_2) λ_{max} (nm) (ε, L·m^{-1}·cm^{-1}): 588 (8.47×10^3), 550 (7.92×10^3), 312 (8.44×10^3), 371 (2.48×10^4). ^{1}H NMR (500 MHz, $CDCl_3$) δ (ppm): 7.00 (t, J = 5.6 Hz, 1H), 5.55 (s,1H), 3.77 (s, 3H), 3.71 (s, 3H), 3.70 (s, 3H), 3.69 (s, 3H), 3.68 (s, 3H), 3.64 (s, 3H), 3.61−3.55 (m, 8H), 3.55 (s, 1H), 3.53 (s, 1H), 3.52 (d, J = 4.4 Hz, 1H), 3.50 (m, 2H), 3.43 (m, 1H), 3.38 (t, J = 6.5 Hz, 3H), 3.00 (m, 1H), 2.94 (m, 1H), 2.83 (m, 1H), 2.79 (t, J = 6.5 Hz, 3H), 2.62 (m, 2H), 2.59−2.52 (m, 3H), 2.51−2.44 (m, 4H), 2.44−2.34 (m, 3H), 2.31 (m, 1H), 2.28 (bs, 1H), 2.25 (m, 1H), 2.23 (s, 3H), 2.20 (bs, 1H), 2.17 (bs, 2H), 2.10 (s, 3H), 1.81 (m, 2H), 1.77 (s, 3H), 1.71 (t, J = 6.5 Hz, 3H), 1.66 (t, J = 6.9 Hz, 3H), 1.51 (s, 3H), 1.38 (s, 3H), 1.37 (s, 3H), 1.27 (s, 3H), 1.21 (s, 3H). ^{13}C NMR (125 MHz, $CDCl_3$) δ (ppm): 175.9, 175.8, 175.3, 173.9, 173.6, 172.9, 172.5, 171.7, 171.5, 171.4, 169.7, 163.6, 161.7, 106.3, 102.2, 91.4, 82.6, 74.6, 70.5, 70.08, 70.05, 69.5, 68.9, 58.4, 58.2, 56.6, 53.5, 52.4, 51.92, 51.85, 51.62, 51.61, 51.2, 46.9, 46.8, 46.0, 41.7, 39.6, 39.2, 37.0, 33.7, 32.9, 32.4, 31.8, 31.4, 30.9, 30.8, 29.6, 29.3, 25.9, 25.7, 24.9, 22.0, 19.8, 19.3, 18.4, 16.9, 15.4, 15.3

*$(CN)_2$Cby[$(OMe)_6$-c-10-aminodecylamide] (**3i**).* Obtained following the similar procedure as for derivative **3g**, starting from acid **1** (75 mg, 0.07 mmol), compound **3i** was isolated as a purple solid (50 mg, 58% yield). R_f 0.1 (11% MeOH in DCM) Anal. Calcd for $C_{63}H_{93}CoN_8O_{13}$ + $4H_2O$: C 58.14, H 7.82, N 8.61. Found: C 58.31, H 7.83, N, 8.63. HRMS ESI (m/z) calcd for $C_{62}H_{93}CoN_7O_{13}$ 1202.6158 $[M - CN]^+$, found 1202.6186. UV/vis (CH_2Cl_2), λ_{max} (nm) (ε, L·m^{-1}·cm^{-1}): 533 (7.32×10^3), 370 (2.47×10^4), 310 (9.02×10^3). ^{1}H NMR (500 MHz, $CDCl_3$) δ (ppm): 7.00 (t, J = 5.5 Hz, 1H), 5.54 (s, 1H), 3.77 (s, 3H), 3.71 (s, 3H), 3.70 (s, 3H), 3.69 (s, 3H), 3.68 (s, 3H), 3.64 (s, 3H), 3.32 (m, 1H), 3.04 (m, 1H), 2.82 (m, 1H), 2.77 (m, 1H), 2.70 (m, 1H), 2.68 (t, J = 7.1 Hz 2H), 2.61 (bs, 2H), 2.60 (s, 1H), 2.55 (m, 2H), 2.50 (s, 1H), 2.47 (t, J = 8.9 Hz, 3H,), 2.43 (m, 1H), 2.40 (m, 1H), 2.27 (s, 1H), 2.26−2.21 (m, 3H), 2.23 (s, 3H), 2.19 (m, 1H), 2.17 (m, 1H), 2.14 (m, 1H), 2.10 (s, 3H), 2.03 (m, 2H), 1.79 (s, 3H), 1.72 (m, 1H), 1.70−1.62 (m, 6H), 1.51 (s, 3H), 1.41 (m, 2H), 1.37 (s, 3H), 1.36 (s, 3H), 1.32 (m, 2H), 1.27 (s, 3H), 1.24 (m, 4H), 1.21 (s 6H,), 1.18 (m, 4H) ppm. ^{13}C NMR (125 MHz, $CDCl_3$) δ (ppm): 175.9, 175.8, 175.4, 173.9, 173.6, 172.9, 172.5, 171.6, 171.5, 171.4, 169.5, 163.6, 161.4, 106.7, 102.2, 91.4, 82.6, 74.7, 58.7, 58.5, 56.6, 53.5, 52.4, 51.9, 51.9, 51.64, 51.62, 51.4, 47.2, 46.9, 46.1, 42.2, 41.6, 39.8, 39.2, 33.7, 33.6, 32.4, 31.8, 31.5, 30.9, 30.8, 29.6, 29.49, 29.48, 29.4, 29.2, 29.1, 27.0, 26.8, 25.8, 25.7, 24.9, 22.0, 19.8, 19.3, 18.4, 16.9, 15.33, 15.31.

*PpIX Monoester (**4**).* PpIX (80 mg, 0.26 mmol) was dissolved in dry DMF (7 mL) under argon, and the resulting solution was cooled to 0 °C. EDC (136 mg, 0.71 mmol) and DMAP (73 mg, 0.60 mmol) were then added. After 30 min of stirring, a solution of 2-trimethylsililethanol (18 mg, 0.15 mmol) in DMF (1 mL) was added dropwise over a 1 h period. The reaction mixture was allowed to warm to room temperature and then stirred overnight. It was then diluted with a solution of NH_4Cl and extracted with AcOEt. The organic phase was washed with water and brine, dried over Na_2SO_4, filtered, and concentrated in vacuo. The crude product was purified using flash chromatography (gradually from 1 to 3% MeOH in DCM). After precipitation from DCM solution using hexane, compound **4** was obtained as a dark-brown solid (58 mg, 62%). R_f 0.6 (5% MeOH in DCM). Anal. Calcd for $C_{39}H_{46}N_4O_4Si$: C 70.66, H 6. 99, N 8.45. Found: C 70.64, H 7.03, N 8.40. HRMS ESI (m/z) calcd for $C_{39}H_{46}N_4O_4Si$ 663.3361 $[M + H]^+$, found 663.3368. UV/vis (CH_2Cl_2) λ_{max} (nm) (ε, L·m^{-1}·cm^{-1}): 630 (1.03×10^4), 575 (1.37×10^4), 540 (2.31×10^4), 505 (2.86×10^4), 406 (3.32×10^5). ^{1}H NMR (500 MHz, $CDCl_3$) δ (ppm): 9.93 and 9.91 (s, s, 1H), 9.85 and 9.84 (s, s, 1H), 9.78 and 9.76 (bs, 2H), 8.14 (dd, J = 11.6 and 17.6 Hz, 1H), 8.04 (m, 1H), 6.26 (dd, J = 10.6 and 17.6 Hz, 2H), 6.11 (dd, J = 4.3 and 11.6 Hz, 2H), 4.25−4.15 (m, 6H), 3.54 and 3.52 (s, s, 3H), 3.51 and 3.50 (s, s, 3H), 3.49 and 3.48 (s, s, 3H), 3.46 and 3.45 (s, s, 3H), 3.20 (t, J = 7.1 Hz, 2H), 3.09 (t, J = 7.8 Hz, 2H), 0.84 (t, J = 8.5 Hz, 2H), −0,09 (s, 9H), −4.23 (bs, 2H). ^{13}C NMR (125 MHz, $CDCl_3$) δ (ppm): 176.0, 174.5, 136.4, 130.2, 130.2, 120.5, 97.6, 97.2, 96.8, 96.1, 63.4, 37.4, 36.8, 22.0, 21.6, 17.2, 12.58, 12.56, 11.6, 11.5, −1.4, −1.7.

*General Procedure for Preparation of Compounds **5a**−**5e**.* PpIX monoester **4** (1 equiv) was dissolved in dry DCM (0.01 M) under argon atmosphere and cooled down to 0 °C. EDC (3 equiv) and DMAP (3 equiv) were added in one portion followed by stirring for 30

dx.doi.org/10.1021/jm400715h | J. Med. Chem. XXXX, XXX, XXX−XXX

min. Then compound **2** (3 equiv) was added in one portion, and the mixture was allowed to warm to room temperature and stirred overnight. The reaction mixture was diluted with DCM, washed 3 times with water, dried over Na_2SO_4, and concentrated under reduced pressure. The crude product was isolated using flash chromatography (1% MeOH in DCM). The most intensive band was collected, concentrated, precipitated with pentane, and centrifuged. Obtained dark-brown solid was dried overnight under reduced pressure.

Compound ***5a***. Starting from monoester **4** (30 mg, 0.05 mmol), compound **5a** was isolated as a brown solid (33 mg, 96% yield). R_f 0.7 (1% MeOH in DCM). Anal. Calcd for $C_{43}H_{53}N_7O_5Si$: C 66.55, H 6.88, N 12.63. Found: C 66.70, H 6.92, N 12.47. MS ESI (m/z): calcd for $C_{43}H_{54}N_7O_5Si$ $[M + H]^+$ 776.39, found 776.40. UV/vis (CH_2Cl_2), λ_{max} (nm) (ε, $L{\cdot}m^{-1}{\cdot}cm^{-1}$): 631 ($9.31 \times 10^3$), 576 ($7.35 \times 10^3$), 540 ($1.12 \times 10^4$), 505 ($1.33 \times 10^4$), 406 ($1.72 \times 10^5$). ^1H NMR (500 MHz, $CDCl_3$) δ (ppm): 9.96 and 9.95 (s, s, 1H), 9.91 (s, 1H), 9.87 (s, 1H), 9.81 and 9.80 (s, s, 1H), 8.23–8.02 (m, 2H), 6.36–6.23 (m, 2H), 6.19–6.08 (m, 2H), 4.42–4.28 (m, 4H), 4.25–4.18 (m, 2H), 4.18–4.12 (m, 2H), 3.58 and 3.57 (s, s, 3H), 3.56 (s, 3H), 3.55 and 3.54 (s, s, 3H), 3.53 (s, 3H), 3.31–3.19 (m, 6H), 2.94 (t, J = 4.5 Hz, 2H), 2.62 (t, J = 4.5 Hz, 2H), 0.92–0.85 (m, 2H), −0.03 and −0.04 (s, s, 9H), −4.20 (bs, 2H). ^{13}C NMR (125 MHz, $CDCl_3$) δ (ppm): 173.2, 173.0, 130.2, 120.5, 97.7, 97.1, 96.8, 96.0, 69.4, 68.7, 63.4, 62.7, 50.0, 37.3, 36.9, 21.8, 21.7, 17.2, 12.6, 11.62, 11.60, 11.58, −1.6.

Compound ***5b***. Starting from monoester **4** (30 mg, 0.05 mmol), compound **5b** was isolated as a brown solid (31 mg, 85% yield). R_f 0.7 (1% MeOH in DCM). Anal. Calcd for $C_{45}H_{57}N_7O_6Si$: C 65.91, H 7.01, N 11.96. Found: C 65.72, H 7.22, N 11.63. MS ESI (m/z): calcd for $C_{45}H_{58}N_7O_6Si$ $[M + H]^+$ 820.41, found 820.42. UV/vis CH_2Cl_2, λ_{max} (nm) (ε, $L{\cdot}m^{-1}{\cdot}cm^{-1}$): 630 ($1.03 \times 10^4$), 576 ($7.76 \times 10^3$), 540 ($1.12 \times 10^4$), 504 ($1.58 \times 10^4$), 406 ($1.83 \times 10^5$). ^1H NMR (500 MHz, $CDCl_3$) δ (ppm): 9.88 and 9.86, (s, s, 1H), 9.81 (s, 1H), 9.89 (s, 1H), 9.72 and 9.69 (s, s, 1H), 8.16–8.00 (m, 2H), 6.62–6.19 (m, 2H), 6.16–6.05 (m, 2H), 4.36–4.24 (m, 4H), 4.23–4.15 (m, 2H), 4.14–4.04 (m, 2H), 3.52 and 3.51 (s, s, 3H), 3.50 and 3.49 (s, s, 3H), 3.48 (s, 3H), 3.45 (s, 3H), 3.29–3.16 (m, 6H), 2.89–2.77 (m, 6H), 2.64–2.55 (m, 2H), 0.91–0.82 (m, 2H), −0.06 and −0.07 (s, s 9H), −4.35 (bs, 2H). ^{13}C NMR (125 MHz, $CDCl_3$) δ (ppm): 173.3, 173.1, 130.2, 120.5, 97.6, 97.1, 96.7, 96.0, 69.9, 69.8, 69.2, 68.8, 63.6, 62.8, 50.7, 50.1, 37.3, 36.9, 21.6, 17.3, 12.6, 11.64, 11.60, −1.6.

Compound ***5c***. Starting from monoester **4** (30 mg, 0.05 mmol), compound **5c** was isolated as a brown solid (35 mg, 90% yield). R_f 0.6 (1% MeOH in DCM). Anal. Calcd for $C_{47}H_{61}N_7O_7Si$: C 65.33, H 7.12, N 11.35. Found: C 65.21, H 7.15, N 11.11. MS ESI (m/z): calcd for $C_{47}H_{62}N_7O_7Si$ $[M + H]^+$ 864.44, found 864.45. UV/vis (CH_2Cl_2), λ_{max} (nm) (ε, $L{\cdot}m^{-1}{\cdot}cm^{-1}$): 630 ($1.12 \times 10^4$), 576 ($7.35 \times 10^3$), 540 ($1.12 \times 10^4$), 505 ($1.33 \times 10^4$), 406 ($1.72 \times 10^5$). ^1H NMR (500 MHz, $CDCl_3$) δ (ppm): 9.92 and 9.91 (s, s, 1H), 9.85 (s, 1H), 9.85 (s, 1H), 9.76 and 9.74 (s, s, 1H), 8.22–8.01 (m, 2H), 6.36–6.21 (m, 2H), 6.19–6.06 (m, 2H), 4.40–4.30 (m, 4H), 4.27–4.20 (m, 2H), 4.19–4.14 (m, 2H), 3.35 (s, 3H), 3.54 (s, 3H), 3.53 (s, 3H), 3.51 (s, 3H), 3.39–3.34 (m, 2H), 3.33–3.30 (m, 2H), 3.30–3.21 (m, 4H), 3.20–3.17 (m, 2H), 3.14 (t, J = 4.9 Hz, 2H), 3.08–3.03 (m, 4H), 2.92–2.86 (m, 2H), 0.95–0.86 (m, 2H), −0.02 and −0.03 (s, s, 9H), −4.29 (bs, 2H). ^{13}C NMR (125 MHz, $CDCl_3$) δ (ppm): 173.2, 173.1, 130.2, 130.1, 120.5, 97.5, 97.0, 96.7, 95.9, 70.1, 70.02, 69.99, 69.94, 69.93, 69.6, 68.8, 63.6, 62.8, 50.4, 37.3, 36.9, 21.8, 21.7, 17.2, 12.5, 11.61, 11.57, −1.6.

Compound ***5d***. Starting from monoester **4** (30 mg, 0.05 mmol), compound **5d** was isolated as a brown solid (33 mg, 95% yield). R_f 0.6 (1% MeOH in DCM). Anal. Calcd for $C_{43}H_{54}N_8O_4Si$: C 66.64, H 7.02, N 14.46. Found: C 66.41, H 6.89, N 14.39. MS ESI (m/z): calcd for $C_{43}H_{55}N_8O_4Si$ $[M + H]^+$ 775.40, found 775.50. UV/vis (CH_2Cl_2), λ_{max} (nm) (ε, $L{\cdot}m^{-1}{\cdot}cm^{-1}$): 630 ($1.04 \times 10^4$), 577 ($6.56 \times 10^3$), 540 ($1.98 \times 10^4$), 505 ($1.33 \times 10^4$), 406 ($2.01 \times 10^5$). ^1H NMR (500 MHz, $CDCl_3$) δ (ppm): 9.82 and 9.79 (s, s, 1H), 9.81 (s, 1H), 9.70 (s, 1H), 9.65 and 9.61 (s, s, 1H), 8.18–8.02 (m, 2H), 6.33–6.21 (m, 2H), 6.17–6.07 (m, 2H), 5.86–5.76 (m, 1H), 4.32–4.18 (m, 4H), 4.05–3.96 (m, 2H), 3.53 and 3.52 (s, s, 3H), 3.51 and 3.50 (s, s, 3H), 3.47 and 3.45 (s, s, 3H), 3.44 and 3.41 (s, s, 3H), 3.20–3.13 (m, 2H), 3.09–3.33 (m, 2H), 3.02–2.97 (m, 2H), 2.46–2.40 (m, 2H), 1.70–1.62 (m, 2H), 1.40–1.33 (m, 2H), 0.70–0.63 (m, 2H), −0.20 and −0.21 (s, s, 9H), −4.58 (bs, 2H). ^{13}C NMR (125 MHz, $CDCl_3$) δ (ppm): 173.6, 172.4, 130.2, 120.4, 97.4, 96.86, 96.83, 96.53, 96.50, 96.2, 69.0, 68.3, 62.7, 49.04, 49.02, 39.6, 38.7, 37.0, 22.8, 21.6, 17.1, 12.6, 12.5, 11.6, 11.5, 11.47, 11.41, −1.8.

Compound ***5e***. Starting from monoester **4** (30 mg, 0.05 mmol), compound **5e** was isolated as a brown solid (32 mg, 98% yield). R_f 0.7 (DCM). Anal. Calcd for $C_{44}H_{52}N_4O_4Si$: C 72.49, H 7.19, N 7.69. Found: C 72.26, H 7.02, N 7.71. MS ESI (m/z): calcd for $C_{44}H_{53}N_4O_4Si$ $[M + H]^+$ 729.38, found 729.30. UV/vis (CH_2Cl_2), λ_{max} (nm) (ε, $L{\cdot}m^{-1}{\cdot}cm^{-1}$): 630 ($8.34 \times 10^3$), 577 ($5.76 \times 10^3$), 540 ($2.17 \times 10^4$), 505 ($1.43 \times 10^4$), 406 ($2.56 \times 10^5$). ^1H NMR (500 MHz, $CDCl_3$) δ (ppm): 10.06 (s, 1H), 1.05 (s, 1H), 9.94 (s, 1H), 9.94 (s, 1H), 8.27–8.15 (m, 2H), 6.39–6.28 (m, 2H), 6.20–6.10 (m, 2H), 4.36 (t, J = 7.8 Hz, 4H), 4.21–4.13 (m, 4H), 3.64 and 3.63 (s, s, 3H), 3.62 and 3.61 (s, s, 3H), 3.58 (s, 3H), 3.57 (s, 3H), 3.25 (t, J = 7.6 Hz, 2H), 3.22 (t, J = 7.6 Hz, 2H), 2.09–2.02 (m, 2H), 1.81 (t, J = 2.7 Hz, 1H), 1.73–1.65 (m, 2H), 0.86–0.79 (m, 2H), −0.09 and −0.10 (s, s, 9H), −3.92 (bs, 2H). ^{13}C NMR (125 MHz, $CDCl_3$) δ (ppm): 173.2, 173.0, 130.3, 120.7, 97.9, 97.3, 97.01, 96.98, 96.1, 82.9, 68.8, 63.1, 62.8, 37.3, 37.0, 27.4, 21.82, 21.79, 17.2, 15.0, 12.67, 12.66, 11.7, −1.64.

General Procedure for Preparation of Porphyrins Zn ***5a–e***. **4** was dissolved in mixture of DCM/MeOH (1/1 v/v, 0.01 M), followed by addition of $Zn(AcO)_2$ (100 equiv). The reaction mixture was stirred for 3 h, diluted with DCM, and washed 3 times with water. Organic phase was dried over Na_2SO_4, concentrated, precipitated with pentane, centrifuged, and dried under reduced pressure. Obtained deep-violet solid was used immediately for the next step without additional purification.

General Procedure for Synthesis of Hybrids ***7–20, 23 and 27***. Compound **2** (1.0 equiv) and porphyrin **Zn5** (1.1 equiv) were dissolved in dry DCM (0.05 M) under argon atmosphere followed by the addition of CuOAc (0.3 equiv). The reaction mixture was stirred vigorously and monitored by TLC. After disappearance of compound **2** (TLC, 40–60 min), the reaction was diluted with DCM, washed with water, dried over Na_2SO_4, and evaporated under reduced pressure. The crude reaction mixture was subjected on flash column, and remaining porphyrin **Zn5** was eluted with 1% MeOH in DCM followed by the elution of hybrid using 5% MeOH/DCM . The isolated product was redissolved in DCM and washed with phosphate buffer (pH = 7.2) containing approximately 1% of NaCN. The organic phase was dried over Na_2SO_4, filtered, and concentrated under reduced pressure and centrifuged. The obtained solid was dried under reduced pressure and dissolved in dry DCM (6 mL), followed by the addition of TFA (2 mL). Reaction mixture was stirred for 4 h, diluted with DCM, and then washed twice with water and then with phosphate buffer (pH = 7.2) containing approximately 1% of NaCN. The organic phase was dried over Na_2SO_4 and concentrated. The hybrid product was purified using flash chromatography (2–7% MeOH in DCM). The most intensive band was collected, concentrated, redissolved in DCM, washed with phosphate buffer (pH = 7.2) containing approximately 1% of NaCN, dried over Na_2SO_4, concentrated, and precipitated with pentane. The obtained dark-violet solid was dried under reduced pressure at 50 °C.

Hybrid ***8***. Starting from corrin **3a** (45 mg, 0.04 mmol) and porphyrin **Zn5b** (38 mg, 0.04 mmol), compound **8** was isolated as a dark-violet solid (42 mg, 58% yield). R_f 0.4 (5% MeOH in DCM). Anal. Calcd for $C_{96}H_{118}CoN_{13}O_{20} + 2H_2O$: C 61.69, H 6.58, N 9.74. Found: C 61.55, H 6.51, N 9.48. MS ESI (m/z) calcd for $C_{95}H_{118}CoN_{12}O_{20}$ $[M - CN]^+$ 1805.79, found 1806.10; calcd for $C_{96}H_{118}CoN_{13}O_{20}Na$ $[M + Na]^+$ 1854.78, found 1855.0. UV/vis (CH_2Cl_2), λ_{max} (nm) (ε, $L{\cdot}m^{-1}{\cdot}cm^{-1}$): 629 ($4.45 \times 10^3$), 579 ($2.83 \times 10^4$), 542 ($2.34 \times 10^4$), 508 ($1.50 \times 10^4$), 406 ($1.56 \times 10^5$). ^1H NMR (500 MHz, DMSO-d_6, 358 K) δ (ppm): 10.20 (s, 1H), 10.16 (s, 1H), 10.14 (s, 2H), 8.42–8.29 (m, 2H), 7.80 (s, 1H), 6.47–6.35 (m, 2H), 6.24–6.16 (m, 2H), 5.66 (s, 1H), 5.08 (d, J = 4.1 Hz, 2H), 4.40–4.27 (m, 4H), 4.20 (t, J = 5.0 Hz, 2H), 4.13–4.03 (m, 2H), 3.68 (s, 3H), 3.67 (s, 3H), 3.66 (s, 3H), 3.63 (s, 3H), 3.60 (s, 3H), 3.61 (s, 3H), 3.60 (s, 3H), 3.58 (s, 3H), 3.57 (s, 3H), 3.53 (s, 3H), 3.52 (s, 3H),

dx.doi.org/10.1021/jm400715h | J. Med. Chem. XXXX, XXX, XXX–XXX

3.50−3.42 (m, 4H), 3.38−3.34 (m, 2H), 3.31−3.25 (m, 2H), 3.23−3.16 (m, 3H), 3.15−3.11 (m, 2H), 3.08−3.05 (m, 2H), 2.90−2.85 (m, 1H), 2.73 (dd, J = 16.3 and 7.5 Hz, 2H), 2.67−2.59 (m, 2H), 2.58−2.50 (m, 4H), 2.45−2.09 (m, 6H), 2.08 (s, 3H), 2.05 (s, 3H), 2.01−1.72 (m, 4H), 1.64−1.49 (m, 2H), 1.46 (s, 3H), 1.34 (s, 3H), 1.28 (s, 3H), 1.20 (s, 3H), 1.11 (s, 3H), 0.96 (s, 3H), −3.81 (bs, 2H). ^{13}C NMR (125 MHz, DMSO, 358 K) δ (ppm): 175.1, 174.6, 174.5, 173.1, 172.5, 172.2, 171.9, 171.7, 171.5, 170.9, 170.2, 169.0, 162.4, 162.3, 141.1, 136.8, 136.0, 129.6, 124.0, 120.5, 102.87, 101.2, 97.2, 96.8, 96.6, 96.3, 89.8, 81.8, 73.9, 68.93, 68.85, 67.9, 67.7, 62.8, 57.4, 57.0, 56.1, 53.4, 52.5, 51.3, 51.0, 50.8, 50.6, 48.8, 47.8, 45.9, 45.3, 41.7, 40.9, 36.2, 36.0, 32.7, 31.4, 30.4, 30.24, 30.17, 21.0, 28.8, 25.6, 24.9, 24.0, 21.0, 20.8, 18.5, 18.4, 17.0, 15.7, 14.6, 14.1, 11.8, 10.7.

Hybrid ***9***. Starting from corrin **3a** (45 mg, 0.04 mmol) and porphyrin **Zn5c** (41 mg, 0.04 mmol), compound **9** was isolated as a dark-violet solid (45 mg, 61% yield). R_f 0.4 (5% MeOH in DCM). Anal. Calcd for $C_{98}H_{122}CoN_{13}O_{21}$ + $3H_2O$: C 60.95, H 6.68, N 9.43. Found: C 61.26, H 6.37, N 9.19. MS ESI (m/z): calcd for $C_{97}H_{122}CoN_{12}O_{21}$ $[M - CN]^+$ 1849.8, found 1850.1; calcd for $C_{98}H_{122}CoN_{13}O_{21}Na$ $[M + Na]^+$ 1898.8, found 1890.0. UV/vis (CH_2Cl_2), λ_{max} (nm) (ε, L·m^{-1}·cm^{-1}): 630 (3.98×10^3), 580 (2.75×10^4), 542 (2.12×10^4), 508 (1.67×10^4), 406 (1.70×10^5); ^{1}H NMR (500 MHz, DMSO-d_6, 358 K) δ (ppm): 11.79 (bs, 1H), 10.21 (s, 1H), 10.17 (s, 1H), 10.15 (s, 2H), 8.50−8.13 (m, 2H), 7.88 (s, 1H), 6.68−6.12 (m, 4H), 5.66 (s, 1H), 5.11 (d, J = 2.3 Hz, 2H), 4.39−4.24 (m, 4H), 4.14−4.04 (m, 2H), 3.69 (s, 3H), 3.67 (s, 3H), 3.66 (s, 3H), 3.63 (s, 3H), 3.61 (s, 6H), 3.60 (s, 3H), 3.59 and 3.58 (s, s, 3H), 3.54 (s, 3H), 3.53 (s, 3H), 3.39 (t, J = 6.9 Hz, 2H), 3.32−3.26 (m, 2H), 3.24−3.11 (m, 8H), 3.08−3.04 (m, 2H), 2.94−2.89 (m, 1H), 2.73 (dd, J = 16.2 and 7.5 Hz, 2H), 2.68−2.51 (m, 5H), 2.45−2.28 (m, 6H), 2.28−2.11 (m, 6H), 2.09 (s, 3H), 2.07 (s, 3H), 2.02−1.70 (m, 6H), 1.65−1.52 (m, 2H), 1.48 (s, 3H), 1.34 (s, 3H), 1.28 (s, 3H), 1.22 (s, 3H), 1.12 (s, 3H), 0.98 (s, 3H), −3.80 (bs, 2H). High quality ^{13}C NMR spectra were not recorded as prolonged exposure to higher temperature caused compound's decomposition.

Hybrid ***10***. Starting from corrin **3a** (45 mg, 0.04 mmol) and porphyrin **Zn5d** (37 mg, 0.04 mmol), compound **10** was isolated as a dark-violet solid (19 mg, 27% yield). R_f 0.4 (5% MeOH in DCM). Anal. Calcd for $C_{94}H_{115}CoN_{14}O_{18}$ + H_2O: C 62.52, H 6.53, N 10.86. Found: C 62.34, H 6.51, N 10.51. MS ESI (m/z): calcd for $C_{93}H_{115}CoN_{13}O_{18}$ $[M - CN]^+$ 1760.78, found 1760.80; calcd for $C_{94}H_{115}CoN_{14}O_{18}Na$ $[M + Na]^+$ 1809.77, found 1809.90. UV/vis (CH_2Cl_2), λ_{max} (nm) (ε, L·m^{-1}·cm^{-1}): 630 (5.32×10^3), 578 (3.23×10^4), 540 (2.89×10^4), 508 (1.65×10^4), 406 (1.66×10^5). ^{1}H NMR (500 MHz, DMSO-d_6, 358 K) δ (ppm): 14.36 (bs, 1H), 10.21 (s, 1H), 10.16 (s, 1H), 10.13 (s, 1H), 10.09 (s, 1H), 8.42−8.29 (m, 2H), 7.75 (bs, 1H), 7.69 (s, 1H), 6.45−6.34 (m, 2H), 6.24−5.15 (m, 2H), 5.54 (s, 1H), 5.09−5.01 (m, 2H), 4.37−4.24 (m, 4H), 4.03−3.95 (m, 2H), 3.69 (s, 2H), 3.68 (s, 3H), 3.66 and 3.65 (s, s, 3H), 3.64 (s, 3H), 3.62 (s, 6H), 3.59 and 3.56 (s, s, 3H), 3.58 (s, 3H), 3.55 (s, 3H), 3.54 (s, 3H), 3.52−3.48 (m, 2H), 3.38−3.32 (m, 4H), 2.90−2.84 (m 2H), 2.78−2.70 (m, 2H), 2.70−2.52 (m 6H), 2.47−2.36 (m, 6H), 2.36−2.11 (m, 8H), 2.09 (s, 3H), 2.06 (s, 3H), 2.01−1.75 (m, 6H), 1.64−1.49 (m, 2H), 1.46 (s, 3H), 1.36 (s, 3H), 1.30 (s, 3H), 1.21 (s, 3H), 1.13 (s, 3H), 0.95 (s, 3H), −3.89 (bs, 2H). ^{13}C NMR (125 MHz, DMSO-d_6, 358 K) δ (ppm): 175.1, 174.7, 174.5, 172.5, 172.2, 171.73, 171.71, 171.5, 171.4, 170.9, 170.2, 169.0, 162.4, 162.3, 141.1, 136.3, 129.7, 123.9, 120.4, 102.9, 101.2, 97.1, 96.7, 96.6, 96.5, 89.8, 81.8, 73.9, 68.4, 67.6, 57.4, 57.0, 56.1, 53.4, 52.5, 51.4, 51.0, 50.8, 50.6, 50.5 48.6, 47.8, 45.6, 45.3, 38.1, 37.7, 32.7, 31.4, 30.4, 30.24, 30.18, 30.0, 28.9, 25.6, 24.9, 24. 0, 21.6, 21.1, 18.5, 18.4, 17.1, 15.8, 14.7, 14.1, 11.8, 10.73, 10.71.

Hybrid ***13***. Starting from corrin **3b** (46 mg, 0.04 mmol) and porphyrin **Zn5c** (41 mg, 0.04 mmol), compound **13** was isolated as a dark-violet solid (30 mg, 41% yield). R_f 0.4 (5% MeOH in DCM). Anal. Calcd for $C_{100}H_{126}CoN_{13}O_{21}$ + H_2O: C 62.46, H 6.71, N 9.47. Found: C 62.46, H 6.74, N 9.28. MS ESI (m/z): calcd for $C_{99}H_{126}CoN_{12}O_{21}$ $[M - CN]^+$ 1877.85, found 1878.00; calcd for $C_{100}H_{126}CoN_{13}O_{21}Na$ $[M + Na]^+$ 1926.84, found 1926.90. UV/vis (CH_2Cl_2), λ_{max} (nm) (ε, L·m^{-1}·cm^{-1}): 630 (4.78×10^3), 580 (2.91×10^4), 542 (2.33×10^4), 508 (1.67×10^4), 406 (1.82×10^5). ^{1}H NMR (500 MHz, DMSO-d_6, 358 K) δ (ppm): 12.42 (bs, 1H), 10.00 (s, 2H), 9.97 (s, 1H), 9.92 and 9.90 (s, s, 2H), 8.41−8.22 (m, 2H), 7.57 (s, 1H), 6.42−6.29 (m, 2H), 6.22−6.08 (m, 2H), 5.60 (s, 1H), 4.35−4.16 (m, 6H), 4.05 (bs, 2H), 3.99 (t, J = 6.9 Hz, 2H), 3.67 (s, 3H), 3.63 (s, 3H), 3.61 (s, 3H), 3.60 (s, 3H), 3.58 (s, 3H), 3.57 and 3.56 (s, s, 3H), 3.52 (s, 6H), 3.52 (s, 3H), 3.50 and 3.49 (s, 3H), 3.28−3.09 (m, 10H), 3.04−2.99 (m, 2H), 2.99−2.95 (m, 2H), 2.87−2.82 (m, 2H), 2.81−2.74 (m, 2H), 2.70−2.53 (m, 8H), 2.47−2.12 (m, 12H), 2.10 (s, 3H), 1.99 (s, 3H), 1.95−1.62 (m, 6H), 1.57−1.51 (m, 2H), 1.49 (s, 3H), 1.30 (s, 3H), 1.26 (s, 3H), 1.16 (s, 3H), 1.11 (s, 3H), 0.92 (s, 3H), −4.50 (bs, 2H). ^{13}C NMR (125 MHz, DMSO-d_6, 358 K) δ (ppm): 175.5, 174.9, 174.8, 174.0, 173.1, 172.9, 172.5, 172.4, 172.3, 172.2, 171.5, 170.6, 169.9, 162.8, 162.4, 145.6, 129.9, 122.0, 120.8, 103.2, 101.6, 97.3, 97.0, 96.7, 96.6, 90.2, 82.1, 74.0, 69.3, 69.1, 68.4, 68.0, 63.5, 63.3, 57.6, 56.2, 53.4, 52.4, 51.9, 51.6, 51.6, 51.4, 51.2, 49.0, 47.9, 46.1, 45.2, 41.8, 41.0, 36.9, 36.4, 33.0, 31.4, 30.7, 30.5, 30.4, 30.3, 29.1, 27.7, 25.9, 25.2, 24.2, 21.7, 21.4, 21.2, 21.1, 18.9, 18.8, 17.4, 16.1, 15.2, 14.7, 13.9, 12.5, 11.2.

Hybrid ***14***. Starting from corrin **3b** (45 mg, 0.04 mmol) and porphyrin **Zn5d** (37 mg, 0.04 mmol), compound **14** was isolated as a dark-violet solid (43 mg, 60% yield). R_f 0.4 (5% MeOH in DCM). Anal. Calcd for $C_{96}H_{119}CoN_{14}O_{18}$ + H_2O: C 62.87, H 6.65, N 10.69. Found: C 62.55, H 6.71, N 10.45. MS ESI (m/z): calcd for $C_{95}H_{119}CoN_{13}O_{18}$ $[M - CN]^+$ 1788.81, found 1789.00; calcd for $C_{96}H_{119}CoN_{14}O_{18}Na$ $[M + Na]^+$ 1837.81, found 1837.90. UV/vis (CH_2Cl_2), λ_{max} (nm) (ε, L·m^{-1}·cm^{-1}): 630 (6.01×10^3), 580 (3.91×10^4), 542 (3.55×10^4), 508 (2.50×10^4), 406 (1.98×10^5). ^{1}H NMR (500 MHz, DMSO-d_6, 358 K) δ (ppm): 14.30 (bs, 1H), 10.26 (s, 1H), 10.25 (s, 1H), 10.21 (s, 1H), 10.19 (s, 1H), 8.46−8.34 (m, 2H), 7.67 (bs, 1H), 7.31 (s, 1H), 6.48−6.37 (m, 2H), 6.26−6.15 (m, 2H), 5.59 (s, 1H), 4.41−4.28 (m, 4H), 4.02−3.95 (m, 2H), 3.94−3.84 (m, 2H), 3.73 and 3.72 (s, s, 3H), 3.71 and 3.70 (s, s, 3H), 3.69 (s, 3H), 3.64 (s, 3H), 3.63 (s, 6H), 3.62 (s, 3H), 3.61 and 3.60 (s, s, 3H), 3.56 (s, 3H), 3.55 (s, 3H), 3.53−3.45 (m, 4H), 3.25−3.16 (m, 4H), 3.16−3.11 (m, 6H), 2.95−2.90 (m, 3H), 2.90 −2.71 (m, 2H), 2.71−2.52 (m, 5H), 2.48−2.33 (m, 6H), 2.24−2.13 (m, 4H), 2.12 (s, 3H), 2.09 (s, 3H), 1.84−1.76 (m, 4H), 1.67−1.53 (m, 3H), 1.49 (s, 3H), 1.36 (s, 3H), 1.31 (s, 3H), 1.23 (s, 3H), 1.14 (s, 3H), 0.99 (s, 3H), −3.73 (bs, 2H). High quality ^{13}C NMR spectra were not recorded as prolonged exposure to higher temperature caused compound's decomposition.

Hybrid ***19***. Starting from corrin **3d** (45 mg, 0.04 mmol) and porphyrin **Zn5a** (37 mg, 0.04 mmol), compound **19** was isolated as a dark-violet solid (51 mg, 70% yield). R_f 0.4 (5% MeOH in DCM). Anal. Calcd for $C_{96}H_{119}CoN_{14}O_{18}$ + $2H_2O$: C 62.26, H 6.69, N 10.59. Found: C 62.45, H 6.85, N 10.23. MS ESI (m/z): calcd for $C_{95}H_{119}CoN_{13}O_{18}$ $[M - CN]^+$ 1788.81, found 1788.90; calcd for $C_{96}H_{119}CoN_{14}O_{18}Na$ $[M + Na]^+$ 1837.81, found 1837.90. UV/vis (CH_2Cl_2), λ_{max} (nm) (ε, L·m^{-1}·cm^{-1}): 630 (4.38×10^3), 579 (4.87×10^4), 542 (2.73×10^4), 508 (1.76×10^4), 406 (1.45×10^5). ^{1}H NMR (500 MHz, DMSO-d_6, 358 K) δ (ppm): 10.16 (s, 1H), 10.13 (s, 1H), 10.10 (s, 2H), 8.40−8.21 (m, 2H), 7.60−7.52 (m, 1H), 7.34 (s, 1H), 6.44−6.35 (m, 2H), 6.22−6.12 (m, 2H), 5.52 (s, 1H), 4.39 − 4.25 (m, 4H), 4.11−4.04 (m, 2H), 4.05−4.00 (m, 2H), 3.68 (s, 3H), 3.67 (s, 3H), 3.63 (s, 3H), 3.62 and 3.61 (s, s, 3H), 3.60 (s, 3H), 3.59 (s, 3H), 3.57 (s, 3H), 3.55 (s, 3H), 3.54 (s, 3H), 5.53 (s, 3H), 3.49−3.46 (m, 2H), 3.42−3.37 (m, 2H), 3.30−3.14 (m, 6H), 3.13−3.04 (m, 2H), 2.93−2.83 (m, 2H), 2.77−2.69 (m, 2H), 2.68−2.51 (m, 4H), 2.46−2.08 (m, 11H), 2.07 (s, 3H), 2.06 (s, 3H), 1.96−1.70 (m, 6H), 1.67−1.53 (m, 4H), 1.48 (s, 3H), 1.34 (s, 3H), 1.28 (s, 3H), 1.20 (s, 3H), 1.12 (s, 3H), 0.97 (s, 3H), −3.87 (bs, 2H). ^{13}C NMR (125 MHz, DMSO-d_6, 358 K) δ (ppm): 174.9, 174.7, 174.4, 173.1, 172.5, 172.3, 171.8, 171.7, 171.5, 171.0, 170.9, 168.4, 162.5, 162.4, 145.6, 136.7, 136.0, 135.8, 129.6, 121.2, 120.5, 103.6, 101.1, 97.2, 96.8, 96.6, 96.3, 90.1, 81.8, 73.8, 68.1, 67.7, 62.7, 57.4, 56.0, 54.6, 52.5, 51.3, 51.0, 50.9, 50.8, 50.6, 49.1, 48.4, 45.8, 45.4, 43.7, 41.0, 37.9, 36.2, 36.0, 32.7, 31.6, 30.6, 30.4, 30.2, 28.8, 28.1, 27.9, 27.8, 25.5, 24.9, 24.0, 22.1, 21.4, 21.0, 20.9, 20.8, 18.5, 17.8, 17.0, 15.8, 14.6, 14.2, 13.2, 11.8, 10.7.

Hybrid ***20***. Starting from corrin **3d** (45 mg, 0.04 mmol) and porphyrin **Zn5b** (38 mg, 0.04 mmol), compound **20** was isolated as a

dx.doi.org/10.1021/jm400715h | J. Med. Chem. XXXX, XXX, XXX−XXX

dark-violet solid (41 mg, 56% yield). R_f 0.4 (5% MeOH in DCM). Anal. Calcd for $C_{98}H_{123}CoN_{14}O_{19}$ + $2H_2O$: C 62.08, H 6.75, N 10.34. Found: C 61.83, H 6.85, N 10.03. MS ESI (m/z): calcd for $C_{97}H_{123}CoN_{13}O_{19}$ $[M - CN]^+$ 1832.84, found 1833.4. UV/vis (CH_2Cl_2), λ_{max} (nm) (ε, $L{\cdot}m^{-1}{\cdot}cm^{-1}$): 630 ($5.22 \times 10^3$), 580 ($2.84 \times 10^4$), 543 ($4.43 \times 10^4$), 508 ($2.32 \times 10^4$), 406 ($2.01 \times 10^5$). ^1H NMR (500 MHz, DMSO-d_6, 358 K) δ (ppm): 10.09 (s, 1H), 10.08 (s, 2H), 10.05 (s, 1H), 8.36−8.25 (m, 2H), 7.36 (t, J = 5.5 Hz, 1H), 7.45 (s, 1H), 6.41−6.31 (m, 2H), 6.22 (m, 2H), 5.66 (s, 1H), 4.37−4.25 (m, 4H), 4.13 (t, J = 5.3 Hz, 2H), 4.10−4.05 (m, 2H), 3.68 (s, 3H), 3.63 (s, 6H), 3.61 (s, 9H), 3.57 (s, 3H), 3.56 (s, 3H), 3.55 (s, 3H), 3.54 (s, 3H), 3.44−3.39 (m, 2H), 3.37−3.33 (m, 2H), 3.32−3.24 (m, 4H), 3.20−3.09 (m, 4H), 2.96−2.87 (m, 4H), 2.78−2.70 (m, 2H), 2.68−2.51 (m, 4H), 2.45−2.25 (m, 11H), 2.25−2.11 (m, 2H), 2.09 (s, 3H), 2.06 (s, 3H), 1.98−1.86 (m, 4H), 1.86−1.72 (m, 2H), 1.68−1.56 (m, 4H), 1.51 (s, 3H), 1.35 (s, 3H), 1.29 (s, 3H), 1.22 (s, 3H), 1.13 (s, 3H), 0.99 (s, 3H), −3.98 (bs, 2H). ^{13}C NMR (125 MHz, DMSO-d_6, 358 K) δ (ppm): 174.9, 174.7, 174.5, 172.5, 172.3, 171.8, 171.7, 171.5, 171.1, 170.9, 168.5, 162.5, 162.4, 136.7, 129.61, 129.58, 121.2, 120.4, 103.6, 101.0, 97.1, 96.6, 96.5, 96.2, 90.1, 81.8, 73.8, 68.9, 68.8, 68.0, 67.7, 62.8, 57.4, 56.0, 54.7, 52.5, 51.3, 51.0, 50.9, 50.8, 50.6, 49.2, 48.6, 45.8, 45.4, 43.7, 41.0, 37.9, 36.0, 32.7, 31.4, 30.4, 30.2, 28.8, 28.2, 25.6, 24.9, 24.0, 22.2, 21.0, 20.8, 18.5, 17.9, 17.0, 15.8, 14.6, 14.7, 11.7, 10.7.

Hybrid ***21***. Starting from corrin **3d** (45 mg, 0.04 mmol) and porphyrin **Zn5c** (38 mg, 0.04 mmol), compound **21** was isolated as a dark-violet solid (29 mg, 39% yield). R_f 0.4 (5% MeOH in DCM). Anal. Calcd for $C_{100}H_{127}CoN_{14}O_{20}$ + $2H_2O$: C 61.91, H 6.81, N 10.11. Found: C 62.04, H 6.54, N 9.97. MS ESI (m/z): calcd for $C_{99}H_{127}CoN_{13}O_{20}$ $[M - CN]^+$ 1876.89, found 1877.00. UV/vis (CH_2Cl_2), λ_{max} (nm) (ε, $L{\cdot}m^{-1}{\cdot}cm^{-1}$): 630 ($4.45 \times 10^3$), 580 ($2.83 \times 10^4$), 541 ($2.34 \times 10^4$), 508 ($2.13 \times 10^4$), 406 ($1.78 \times 10^5$). ^1H NMR (500 MHz, DMSO-d_6, 358 K) δ (ppm): 14.37 (bs, 1H), 10.27 (s, 1H), 10.21 (s, 1H), 10.20 (s, 1H), 10.18 (s. 1H), 8.45−8.29 (m, 2H), 7.65 (t, J = 5.5 Hz, 1H), 7.52 (s, 1H), 6.48−6.37 (m, 2H), 6.24−6.16 (m, 2H), 5.57 (s, 1H), 4.40−4.30 (m, 4H), 4.24 (t, J = 5.5 Hz, 2H), 4.12−4.05 (m, 2H), 3.72 and 3.71 (s, s, 3H), 3.70 and 3.69 (s, s, 3H), 3.67 (s, 3H), 3.64 (s, 3H), 3.63 (s, 3H), 3.61 (s, 3H), 3.60 (s, 3H), 3.59 and 3.57 (s, s, 3H), 3.54 (s, 3H), 3.53 (s, 3H), 3.39−3.32 (m, 4H), 3.29 (t, J = 7.2 Hz, 2H), 3.22−3.09 (m, 4H), 2.74 (dd, J = 16.1 and 7.5 Hz, 2H), 2.68−2.54 (m, 6H), 2.45−2.26 (m, 10H), 2.25−2.11 (m, 5H), 2.10 (s, 3H), 2.09 (s, 3H), 2.06−1.73 (m, 12H), 1.67−1.60 (m, 4H), 1.51 (s, 3H), 1.35 (s, 3H), 1.29 (s, 3H), 1.23 (s, 3H), 1.13 (s, 3H), 1.01 (s, 3H), −3.72 (bs, 2H). ^{13}C NMR (125 MHz, DMSO-d_6, 358 K) δ (ppm): 175.5, 174.9, 174.8, 174.0, 173.1, 172.9, 172.5, 172.4, 172.3, 172.2, 171.5, 170.6, 169.9, 162.8, 162.4, 145.6, 129.9, 122.0, 120.8, 103.2, 101.6, 97.3, 97.0, 96.7, 96.6, 90.2, 82.1, 74.0, 69.3, 69.1, 68.4, 68.0, 63.5, 63.3, 57.6, 56.2, 53.4, 52.4, 51.9, 51.6, 51.6, 51.4, 51.2, 49.0, 47.9, 46.1, 45.2, 41.8, 41.0, 36.9, 36.4, 33.0, 31.4, 30.7, 30.5, 30.4, 30.3, 29.1, 27.7, 25.9, 25.2, 24.2, 21.7, 21.4, 21.2, 21.1, 18.9, 18.8, 17.4, 16.1, 15.2, 14.7, 13.9, 12.5, 11.2.

Hybrid ***22***. Starting from corrin **3d** (45 mg, 0.04 mmol) and porphyrin **Zn5d** (37 mg, 0.04 mmol), compound **22** was isolated as a dark-violet solid (57 mg, 79% yield). R_f 0.3 (5% MeOH in DCM). Anal. Calcd for $C_{96}H_{120}CoN_{15}O_{17}$ + $2H_2O$: C 62.29, H 6.75, N 11.35. Found: C 62.11, H 6.82, N 11.07. MS ESI (m/z) calcd for $C_{95}H_{120}CoN_{14}O_{17}$ $[M - CN]^+$ 1787.83, found 1787.90. UV/vis (CH_2Cl_2), λ_{max} (nm) (ε, $L{\cdot}m^{-1}{\cdot}cm^{-1}$): 630 ($4.45 \times 10^3$), 580 ($2.83 \times 10^4$), 541 ($2.34 \times 10^4$), 508 ($1.50 \times 10^4$), 406 ($1.60 \times 10^5$). ^1H NMR (500 MHz, DMSO-d_6, 358 K) δ (ppm): 14.40 (bs, 1H), 10.19, (s, 1H), 10.13 (s, 1H), 10.10 (s, 1H), 10.06 (s, 1H), 8.39 (m, 2H), 7.84 (bs, 1H), 7.61 (bs, 1H), 7.29 (s, 1H), 6.43−6.35 (m, 2H), 6.22−6.13 (m, 2H), 5.52 (s, 1H), 4.34−4.19 (m, 4H), 3.93−2.85 (m, 2H), 3.67 (s, 3H), 3.66 and 3.65 (s, s, 3H), 3.64 (s, 3H), 3.63 (s, 3H), 3.60 (s, 3H), 3.59 (s, 3H), 3.56 (s, 3H), 3.55 (s, 3H), 3.54 (s, 6H), 3.51−3.46 (m, 3H), 3.32−3.26 (m, 4H), 3.10−3.00 (m, 5H), 2.94−2.82 (m, 4H), 2.78−2.69 (m, 2H), 2.68−2.51 (m 4H), 2.45−2.40 (m, 4H), 2.38−2.34 (m, 3H), 2.33−2.09 (m, 6H), 2.08 (s, 3H), 2.07 (s, 3H), 1.96−1.71 (m, 4H), 1.65−1.53 (m, 4H), 1.48 (s, 3H), 1.34 (s, 3H), 1.29 (s, 3H), 1.21 (s, 3H), 1.13 (s, 3H), 0.97 (s, 3H), −3.92 (bs, 2H). ^{13}C NMR (500 MHz, DMSO-d_6, 358 K) δ (ppm): 174.9, 174.7, 174.5, 172.5, 172.3, 171.7, 171.6, 171.0, 170.9, 168.5, 162.5, 162.4, 129.7, 121.2, 120.4, 103.6, 96.8, 96.6, 96.2, 90.1, 81.8, 73.8, 68.4, 67.7, 57.4, 56.0, 52.5, 51.3, 51.0, 50.8, 50.6, 49.1, 48.4, 45.8, 45.4, 38.1, 37.9, 32.7, 31.4, 30.4, 30.2, 28.8, 28.2, 25.5, 25.0, 24.0, 22.1, 21.7, 21.0, 18.5, 17.8, 17.0, 15.8, 14.6, 14.2, 11.8, 10.7.

Hybrid ***23***. Starting from corrin **3e** (48 mg, 0.04 mmol) and porphyrin **Zn5e** (35 mg, 0.04 mmol), compound **23** was isolated as a dark-violet solid (54 mg, 73% yield). R_f 0.4 (5% MeOH in DCM). Anal. Calcd for $C_{98}H_{122}CoN_{13}O_{20}$ + $2H_2O$: C 62.05, H 6.69, N 9.60. Found: C 62.12, H 6.92, N 9.44. MS ESI (m/z): calcd for $C_{97}H_{122}CoN_{12}O_{20}$ $[M - CN]^+$ 1833.82, found 1833.80; calcd for $C_{98}H_{122}CoN_{13}O_{20}Na$ $[M + Na]^+$ 1882.82, found 1882.70. UV/vis (CH_2Cl_2), λ_{max} (nm) (ε, $L{\cdot}m^{-1}{\cdot}cm^{-1}$): 630 ($3.97 \times 10^3$), 580 ($2.01 \times 10^4$), 542 ($2.55 \times 10^4$), 508 ($1.86 \times 10^4$), 406 ($1.72 \times 10^5$). ^1H NMR (500 MHz, DMSO-d_6, 358 K) δ (ppm): 14.30 (bs, 1H), 10.20 (s, 1H), 10.12 and 10.10 (s, s, 1H), 10.07 (s, 1H), 10.04 (s, 1H), 8.47−8.17 (m, 2H), 7.22 (s, 1H), 6.46 (m, 2H), 6.21 (m, 2H), 5.56 (s, 1H), 4.39−4.14 (m, 4H), 4.11−3.99 (m, 4H), 3.70 and 3.69 (s, s, 3H), 3.68 (s, 3H), 3.63 (s, 6H), 3.62 (s, 3H), 3.60 (s, 3H), 3.57 (s, 3H), 3.55 (s, 3H), 3.54 (s, 3H), 3.53 (s, 3H), 3.47−3.01 (m, 15H), 2.79−2.67 (m, 4H), 2.64−2.51 (m, 4H), 2.45−2.14 (m, 12H), 2.10 (s, 3H), 2.05 (s, 3H), 2.00−1.84 (m, 4H), 1.83−1.55 (m, 6H), 1.49 (s, 3H), 1.35 (s, 3H), 1.29 (s, 3H), 1.22 (s, 3H), 1.12 (s, 3H), 0.98 (s, 3H), −3.97 (bs, 2H). High quality ^{13}C NMR spectra were not recorded as prolonged exposure to higher temperature caused compound's decomposition.

Hybrid ***27***. Starting from corrin **26** (47 mg, 0.04 mmol) and porphyrin **Zn5b** (38 mg, 0.04 mmol), compound **27** was isolated as a dark-violet solid (48 mg, 64% yield). R_f 0.4 (5% MeOH in DCM). Anal. Calcd for $C_{99}H_{123}CoN_{14}O_{21}$ + $2H_2O$: C 61.29, H 6.60, N 10.11. Found: C 61.03, H 6.75, N 10.84. MS ESI (m/z): calcd for $C_{98}H_{123}CoN_{13}O_{21}$ $[M - CN]^+$ 1876.83, found 1876.90; calcd for $C_{99}H_{123}CoN_{14}O_{21}Na$ $[M + Na]^+$ 1925.82, found 1925.90. UV/vis CH_2Cl_2, λ_{max} (nm) (ε, $L{\cdot}m^{-1}{\cdot}cm^{-1}$): ($5.47 \times 10^3$), 574 ($1.29 \times 10^4$), 541 ($1.70 \times 10^4$), 505 ($1.69 \times 10^4$), 406 ($1.48 \times 10^5$). ^1H NMR (500 MHz, DMSO-d_6, 358 K) δ (ppm): 10.08 (s, 1H), 10.07 (s, 1H), 10.05 (s, 1H), 10.02 and 10.00 (s, s, 1H), 9.06 (s, 1H), 8.43−8.31 (m, 2H), 7.62 (s, 1H), 6.41−6.30 (m, 2H), 6.22−6.12 (m, 2H), 4.33−4.19 (m, 4H), 4.16−4.09 (m, 2H), 4.06−3.99 (m, 2H), 3.65 (s, 3H), 3.62 (s, 3H), 3.61 (s, 3H), 3.60 (s, 3H), 3.59 (s, 3H), 3.54 (s, 3H), 3.51 (s, 3H), 3.49 (s, 3H), 3.46 (s, 3H), 3.45 (s, 3H), 3.42 (m, 2H), 3.36−3.27 (m, 5H), 3.26−3.21 (m, 4H), 3.20−3.15 (m, 2H), 3.14−3.07 (m, 2H), 3.05−3.00 (m, 2H), 2.94−2.90 (m, 2H), 2.86−2.67 (m, 4H), 2.63−2.51 (m, 4H), 2.45−2.23 (m, 8H), 2.22−2.09 (m, 4H), 2.05 (s, 3H), 2.02−1.85 (m, 6H), 1.82 (s, 3H), 1.75−1.52 (m, 6H), 1.27 (s, 3H), 1.23 (s, 3H), 1.08 (s, 3H), 1.07 (s, 3H), 0.62 (s, 3H), −4.30 (bs, 2H). ^{13}C NMR (500 MHz, DMSO-d_6, 358 K) δ (ppm): 174.7, 173.8, 173.0, 172.8, 172.6, 172.04, 171.97, 171.9, 171.8, 171.4, 171.1, 170.3, 162.9, 161.5, 145.1, 129.6, 129.6, 121.7, 103.7, 103.2, 101.0, 97.0, 96.7, 96.4, 81.7, 73.1, 68.7, 68.6, 67.9, 67.6, 62.8, 56.9, 55.4, 53.1, 51.5, 51.2, 51.0, 50.7, 50.6, 48.4, 46.6, 46.4, 44.8, 36.1, 34.3, 32.5, 30.8, 30.1, 29.8, 29.3, 29.2, 28.6, 24.9, 24.6, 23.9, 21.3, 21.1, 20.7, 20.3, 17.7, 16.6, 15.8, 14.9, 14.4, 13.5, 12.1, 10.8.

Protected Hybrid ***24a***. Compound **3f** (90 mg, 0.08 mmol) and porphyrin **4** (50 mg, 0.08 mmol) were dissolved in dry DMF (0.7 mL), and the solution was cooled to 0 °C. DCC (60 mg, 0.29 mmol) and DMAP (9 mg, 0.07 mmol) were added. After 10 min of stirring in 0 °C, a flask with the reaction mixture was immersed in water inside ultrasonic cleaner (40 kHz) for 2 h. It was then diluted with AcOEt (10 mL) and washed with water (5 × 10 mL). Organic phase was then dried over Na_2SO_4, filtered, and concentrated in vacuo. The crude product was purified using flash chromatography (1−3% MeOH in DCM). The isolated pure product was redissolved in DCM and washed with phosphate buffer (pH = 7.2) containing approximately 1% of NaCN. The organic phase was dried over Na_2SO_4, filtered, and concentrated in vacuo. Precipitation from AcOEt solution using hexane gave hybrid **24a** as a dark-brownish solid (49 mg, 35%). R_f 0.6 (5% MeOH in DCM). Anal. Calcd for $C_{96}H_{124}CoN_{11}O_{18}Si$: C 63.81, H 6.92, N 8.53. Found: C 63.30, H 7.02, N 8.26. HRMS ESI (m/z): calcd for $C_{96}H_{124}CoN_{11}O_{18}SiNa$ $[M + Na]^+$ 1828.8119, found 1828.8132. UV/vis (CH_2Cl_2), λ_{max} (nm) (ε, $L{\cdot}m^{-1}{\cdot}cm^{-1}$): 630 (5.40

dx.doi.org/10.1021/jm400715h | J. Med. Chem. XXXX, XXX, XXX−XXX

× 10^3), 582 (1.50 × 10^4), 542 (1.86 × 10^4), 506 (1.81 × 10^4), 406 (1.60 × 10^5). ^{1}H NMR (500 MHz, $CDCl_3$) δ (ppm): 10.13 (s,1H), 10.11 (s,1H), 10.01 (s,1H), 9.99 (s, 1H), 8.24 (m, 2H), 6.80 (q, J = 6.5 Hz, 1H,), 6.35 (d, J = 17.8, 2H), 6.17 (dd, J = 1.2 and 11.4 Hz, 2H), 5.40 and 5.39 (s, s, 1H), 4.37 (t, J = 6.9 Hz, 4H), 4.25 (m, 4H), 3.71 (s, 3H), 3.68 (s, 3H), 3.68 and 3.67 (s, s, 3H), 3.66 (s, 6H), 3.64 (s, 3H), 3.61 (s, 3H), 3.60 and 3.60 (s, s, 3H), 3.59 (s, 3H), 3.52 and 3.51(s, s, 1H), 3.43 (q, J = 5.0 Hz, 2H), 3.37 (m, 1H), 3.27−3.19 (m, 6H), 2.91−2.83 (m, 2H), 2.76 (m, 1H), 2.65 (m, 1H), 2.56−2.49 (m, 4H), 2.46 (m, 1H), 2.43 (m, 1H), 2.40 (m, 1H), 2.36 (m, 1H), 2.33 (m, 1H), 2.31 (m, 1H), 2.23 (m, 1H), 2.19 (bs, 1H), 2.16 (bs, 1H), 2.14 (bs, 1H), 2.12 (m, 1H), 2.10 (s, 3H), 2.08 (s, 3H), 2.07 (bs, 1H), 2.03 (s, 3H), 2.01−1.92 (m, 2H), 1.73 (m, 1H), 1.67 (s, 3H), 1.63 (s, 3H), 1.57 (m, 1H), 1.45 (s, 3H), 1.31 (s, 3H), 1.23 and 1.22 (s, s, 3H), 1.16 and 1.15 (s, s, 3H), 1.04 and 1.04 (s, s, 3H), 0,81 (m, 2H), −0.11 (s, 9H), −3.81 (s, 2H). ^{13}C NMR (125 MHz, $CDCl_3$) δ (ppm): 175.9, 175.7, 175.2, 173.8, 173.5, 173.2, 173.0, 172.9, 172.5, 171.7, 171.5, 171.3, 169.7, 163.4, 161.6, 130.3, 120.8, 106.1, 102.1, 98.0, 97.4, 97.1, 96.2, 91.2, 82.6, 74.6, 69.0, 68.4, 63.7, 62.8, 58.4, 57.9, 56.6, 53.4, 52.4, 51.83, 51.80, 51.7, 51.6, 51.0, 46.8, 46.5, 45.9, 41.6, 39.1, 38.7, 37.3, 36.8, 33.6, 32.3, 31.6, 31.3, 30.8, 30.7, 29.6, 25.8, 25.6, 24.8, 21.9, 21.8, 21.6, 19.6, 19.2, 18.3, 17.2, 16.9, 15.3, 15.2, 12.7, 11.73, 11.71, −0.03, −1.7.

Protected Hybrid ***24b***. Compound **3g** (70 mg, 0.06 mmol) and poprhyrin **4** (40 mg, 0.06 mmol) were dissolved in dry DMF (7 mL), and the solution was cooled to 0 °C. HBTU (70 mg, 0.18 mmol), HOBt (26 mg, 0.19 mmol), and DIPEA (40 μL, 0.23 mmol) were added. After 30 min, the reaction mixture was allowed to warm to room temperature and then stirred overnight. It was then diluted with AcOEt (20 mL) and washed with phosphate buffer (pH = 7.2) containing approximately 1% of NaCN. The organic phase was then dried over Na_2SO_4, filtered, and concentrated in vacuo. The crude product was purified using flash chromatography (1−3% MeOH in DCM). The isolated pure product **24b** was redissolved in DCM and washed with phosphate buffer (pH = 7.2) containing approximately 1% of NaCN. The organic phase was dried over Na_2SO_4, filtered, and concentrated in vacuo. Precipitation from AcOEt solution using hexane gave hybrid **24b** as a dark-brownish solid (66 mg, 61%). R_f 0.6 (5% MeOH in DCM). Anal. Calcd for $C_{98}H_{129}CoN_{12}O_{18}Si + 2H_2O$: C 62.40, H 7.11, N 8.91. Found: C 62.66, H 7.06, N 8.73. HRMS ESI (m/z): calcd for $C_{98}H_{129}CoN_{12}O_{18}SiNa_2$ 947.4216 $[M + 2Na]^{2+}$, found 947.4213. UV/vis (CH_2Cl_2), λ_{max} (nm) (ε, L·m^{-1}·cm^{-1}): 630 (4.38 × 10^3), 582 (1.44 × 10^4), 407 (1.72 × 10^5), 542 (1.80 × 10^4), 506 (1.73 × 10^4). ^{1}H NMR (500 MHz, $CDCl_3$) δ (ppm): 10.16 (s, 1H), 10.13 and 10.10 (s, s, 1H)10.03 (s, 1.5H), 10.01 (s, 0.5H), 8.27 (m, 2H), 6.57 (m, 2H), 6.37 (dd, J = 7.8 and 17.8 Hz, 2H), 6.20 (bd, J = 11.4 Hz, 2H), 4.85 and 4.84 (s, s, 1H), 4.39 (q, J = 8.1 Hz, 4H), 4.09 (t, J = 8.5 Hz 2H), 3.71 and 3.70 (s, s, 3H), 3.69 (s, 6H), 3.66 (s, 3H), 3.63 (s, 3H), 3.62 and 3.61 (s, s, 3H), 3.60 (s, 3H), 3.59 (s, 3H), 3.58 (s, 3H), 3.49 (m, 2H), 3.45 and 3.43 (s, s, 3H), 3.24 (m, 4H), 3.08 (m, 3H), 2.92 (m, 2H), 2.75 (m, 1H), 2.66 (m, 4H), 2.49−2.41 (m, 4H), 2.39 (m, 2H), 2.35 (m, 2H), 2.30 (m, 1H), 2.27 (m, 1H), 2.22 (m, 1H), 2.18 (m, 3H), 2.09 (bs, 1H), 2.06 (m, 2H), 2.02 (m, 2H), 1.91 (s, 2H), 1.85 (s, 6H), 1.81 (m, 2H), 1.71 (s, 3H), 1.60 (s, 1H), 1.57 (m, 1H), 1.47 (m, 2H), 1.35 (s, 3H), 1.30 (s, 3H), 1.28 (s, 3H), 1.25 (s, 3H), 1.14 (m, 2H), 1.07 and 1.05 (s, s, 3H), 1.02 and 1.00 (s, s, 3H), 0.73 (m, 2H), −0.18 (s, 9H), −3.84 (s, 2H). ^{13}C NMR (125 MHz, $CDCl_3$) δ (ppm): 175.6, 175.1, 173.8, 173.5, 173.3, 172.8, 172.5, 171.6, 171.4, 171.1, 169.6, 163.3, 161.5, 130.2, 120.9, 105.8, 101.9, 97.9, 97.3, 97.0, 96.6, 90.8, 82.4, 74.4, 69.5, 68.9, 68.6, 62.8, 58.2, 57.3, 56.5, 53.2, 52.3, 51.80, 51.76, 51.63, 51.49, 51.5, 50.5, 46.6, 45.9, 45.8, 41.4, 39.3, 39.1, 39.0, 38.5, 37.2, 33.6, 32.2, 31.6, 31.1, 30.6, 30.4, 29.5, 25.5, 25.4, 24.7, 22.6, 22.3, 21.8, 19.4, 18.7, 18.1, 17.1, 16.8, 15.2, 15.0, 12.7, 11.7, 11.6, −1.72.

Protected Hybrid ***24c***. Following the procedure described above for hybrid **24b**, corrin **3h** (55 mg, 0.04 mmol) was reacted with porphyrin **4** (29 mg, 0.04 mmol) giving hybrid **24c** as a dark-brownish solid (52 mg, 64% yield). R_f 0.5 (5% MeOH in DCM) Anal. Calcd for $C_{102}H_{137}CoN_{12}O_{19}Si + 2H_2O$: C 62.56, H 7.26, N 8.58. Found: C 62.67, H 7.22, N, 8.30. LRMS ESI (m/z): calcd for $C_{101}H_{137}CoN_{11}O_{19}Si$ $[M - CN]^+$ 1894.9, found 1894.8. UV/vis (CH_2Cl_2), λ_{max} (nm) (ε, L·m^{-1}·cm^{-1}): 630 (4.18 × 10^3), 583 (1.45 × 10^4), 542 (1.84 × 10^4), 507 (1.74 × 10^4), 407 (1.78 × 10^5). ^{1}H NMR (500 MHz, $CDCl_3$) δ (ppm): 10.16 (s, 1H), 10.11 and 10.10 (s, s, 1H), 10.02 (s, 1H), 10.02 and 10.00 (s, s, 1H), 8.26 (dd, J = 11.5 and 17.8 Hz, 2H), 6.86 (t, J = 5.5 Hz, 1H), 6.48 (m, 1H), 6.37 (bd, J = 17.8 Hz, 2H), 6.19 (dd, J = 1.2 and 11.5 Hz, 2H), 5.28 and 5.27 (s, s, 1H), 4.38 (t, J = 7.1 Hz, 4H), 4.02 (m, 2H), 3.73 (s, 3H), 3.69 (s, 3H), 3.68 (s, 6H), 3.67 (s, 3H), 3.63 (s, 3H), 3.62 (s, 3H), 3.61 and 3.60 (s, s, 3H), 3.59 and 3.58 (s, s, 3H), 3.56 (s, 3H), 3.25−3.17 (m, 6H), 3.09 (m, 4H), 3.06 (m, 2H), 2.97 (m, 2H), 2.87 (m, 1H), 2.76 (t, J = 6.0 Hz, 2H), 2.74 (t, J = 6.0 Hz, 2H), 2.68 (m, 2H), 2.58−2.52 (m, 5H), 2.51−2.46 (m, 2H), 2.41 (m, 2H), 2.38 (bs, 1H), 2.35−2.29 (m, 1H), 2.22 (m, 2H), 2.19 (m, 2H), 2.26 (bs, 1H), 2.13 (m, 2H), 2.09 and 2.08 (s, s, 3H), 2.00 (s, 3H), 1.96 (m, 2H), 1.90 (dd, J = 9.9 and 12.9 Hz, 2H), 1.69 (s, 3H), 1.59 and 1.58 (s, s, 3H), 1.47 (m, 2H), 1.44 (s, 3H), 1.41 (m, 3H), 1.31 (s, 3H), 1.23 (s, 3H), 1.16 and 1.15 (s, s, 3H), 1.05 (s, 3H), 0.64 (m, 2H), −0.23 (s, 9H), −3.85 (s, 2H). ^{13}C NMR (125 MHz, $CDCl_3$,) δ (ppm): 175.8, 175.7, 175.2, 173.8, 173.7, 173.5, 172.8, 172.5, 171.6, 171.4, 171.3, 169.5, 163.4, 161.5, 130.2, 120.8, 106.2, 102.1, 97.9, 97.3, 97.0, 96.54, 96.53, 91.2, 82.6, 74.6, 69.8, 69.63, 69.56, 69.2, 68.7, 68.6, 62.8, 58.4, 58.1, 56.5, 53.4, 52.4, 51.8, 51.8, 51.6, 51.6, 51.0, 46.8, 46.7, 46.0, 41.6, 39.9, 39.1, 37.2, 36.3, 33.6, 32.3, 31.7, 31.3, 30.7, 29.6, 29.1, 28.7, 25.6, 24.8, 23.0, 21.9, 21.8, 19.6, 19.0, 18.3, 17.0, 16.9, 15.3, 15.2, 12.7, 11.7, 11.6, −1.8.

Protected Hybrid ***24d***. Following the procedure described above for hybrid **24b**, corrin **3i** (70 mg, 0.06 mmol) was reacted with porphyrin **4** (39 mg, 0.06 mmol), giving hybrid **24d** as a dark-brownish solid (64 mg, 59% yield); 59% yield. R_f 0.5 (5% MeOH in DCM). Anal. Calcd for $C_{102}H_{137}CoN_{12}O_{16}Si$: C 65.36, H 7.37, N 8.97. Found: C 65.04, H 7.34, N, 8.77. HRMS ESI (m/z): calcd for $C_{102}H_{137}CoN_{12}O_{16}SiNa$ $[M + Na]^+$ 1895.9269, found 1895.9359. UV/vis (CH_2Cl_2), λ_{max} (nm) (ε, L·m^{-1}·cm^{-1}): 630 (5.66 × 10^3), 583 (1.59 × 10^4), 542 (1.95 × 10^4), 506 (1.89 × 10^4), 407 (1.67 × 10^5). ^{1}H NMR (500 MHz, $CDCl_3$) δ (ppm): 10.08 and 10.08 (s, s, 1H), 10.05 and 10.04 (s, s, 1H), 9.94 (s, 1H), 9.93 and 9.92 (s, s, 1H), 8.23 (m, 2H), 6.94 (t, J = 5.6 Hz, 1H), 6.34 (bd, J = 17.8 Hz, 2H), 6.28 (m, 1H), 6.17 (d, J = 11.5 Hz, 2H), 5.43 and 5.43 (s, s, 1H), 4.34 (m, 4H), 3.75 (s, 3H), 3.70 (s, 3H), 3.69 (s, 3H), 3.67 (s, 3H), 3.65 (s, 6H), 3.63 (s, 3H), 3.63 (s, 3H), 3.57 (s, 3H), 3.56 and 3.55 (s, s, 3H), 3.28 (m, 1H), 3.17 (m, 4H), 3.07 (t, J = 8.0 Hz, 2H), 2.95 (t, J = 5.0 Hz, 1H), 2.79 (m, 1H), 2.71 (m, 1H), 2.59 (m, 2H), 2.59−2.49 (m, 4H), 2.48−2.40 (m, 4H), 2.36 (m, 3H), 2.29−2.20 (m, 3H), 2.16 (s, 3H), 2.14 (bs, 2H), 2.09 (m, 1H), 2.06 (s, 3H), 2.05 (m, 1H), 2.00 (m, 3H), 1.78 (m, 1H), 1.73 (s, 3H), 1.69 (m, 1H), 1.66 (s, 3H), 1.59 (m, 1H), 1.48 (s, 3H), 1.35 (s, 3H), 1.30 (s, 3H), 1.26 (m, 2H), 1.21 (s, 3H), 1.13 (s, 3H), 1.08−0.92 (m, 14H), 0.49 (m, 2H), −0.33 (s, 9H), −4.01 (s, 2H). ^{13}C NMR (125 MHz, $CDCl_3$) δ (ppm): 175.8, 175.7, 175.3, 173.9, 173.8, 173.6, 172.9, 172.6, 172.5, 171.6, 171.5, 171.3, 169.4, 163.5, 161.3, 130.3, 120.7, 106.6, 102.1, 97.8, 97.2, 96.9, 96.4, 91.3, 82.6, 74.6, 62.8, 58.6, 58.4, 56.6, 53.5, 52.4, 51.9, 51.8, 51.6, 51.3, 47.2, 46.8, 46.1, 41.6, 40.2, 39.7, 39.6, 39.1, 37.2, 33.7, 32.4, 31.7, 31.4, 30.8, 30.7, 29.6, 29.4, 29.3, 29.24, 29.19, 29.1, 29.0, 26.9, 26.7, 25.73, 25.66, 24.8, 23.3, 22.0, 21.7, 19.7, 19.2, 18.4, 16.9, 16.8, 15.27, 15.26, 12.69, 12.68, 11.67, 11.65, 11.57, 11.55, −1.9.

Hybrid ***25a***. Compound **24a** (40 mg, 0.02 mmol) was dissolved in DCM (0.21 mL), and TFA (0.21 mL) was added. After 2 h of stirring, the reaction mixture was diluted with AcOEt (10 mL) and washed with phosphate buffer (pH = 7.2) containing approximately 1% of NaCN. The organic phase was then dried over Na_2SO_4, filtered, and concentrated in vacuo. The crude product was purified using flash chromatography (1−10% MeOH in DCM). The isolated pure product was redissolved in DCM and washed with phosphate buffer (pH = 7.2) containing approximately 1% of NaCN. The organic phase was dried over Na_2SO_4, filtered, and concentrated in vacuo. Precipitation from AcOEt solution using hexane gave hybrid **25a** as a dark-brownish solid (28 mg, 73%). R_f 0.4 (5% MeOH in DCM). Anal. Calcd for $C_{91}H_{112}CoN_{11}O_{18} + 2H_2O$: C 62.71, H 6.71, N 8.84. Found: C 62.69, H 6.53, N 8.60. HRMS ESI (m/z) calcd for $C_{90}H_{113}CoN_{10}O_{18}$ $[M + H - CN]^{2+}$ 840.3778, found 840.3787. UV/vis (CH_2Cl_2), λ_{max} (nm) (ε,

dx.doi.org/10.1021/jm400715h | J. Med. Chem. XXXX, XXX, XXX−XXX

$L \cdot m^{-1} \cdot cm^{-1}$): 630 ($6.29 \times 10^3$), 577 ($1.68 \times 10^4$), 541 ($2.17 \times 10^4$), 506 ($2.13 \times 10^4$), 406 ($1.83 \times 10^5$). ^{1}H NMR (500 MHz, $CDCl_3$) δ (ppm): 9.99 (bs, 1.5H), 9.97 (s, 0.5 H), 9.92 (s, 1H), 9.87 and 9.84 (s, s, 1H), 8.19 (m, 2H), 7.07 (m, 1H), 6.32 (dd, J = 17.7 Hz, 2H), 6.16 (dd, J = 11.4 Hz, 2H), 5.31 (s, s, 1H), 4.29 (m, 6H), 3.75 (s, 3H), 3.69 and 3.68 (s, s, 3H), 3.67 and 3.67 (s, s, 3H), 3.62 and 3.62 (s, s, 3H), 3.61 (s, 6H), 3.60 (s, 3H), 3.59 and 3.58 (s, s, 3H), 3.56 and 3.55 (s, s, 3H), 3.52 and 3.51 (s, s, 3H), 3.43 (t, J = 5.8 Hz, 2H), 3.20 (t, J = 8.3 Hz, 2H), 3.16 (t, J = 7.9 Hz, 2H), 3.01 (m, 1H), 2.74 (m, 2H), 2.61 (m, 1H), 2.60 (bs, 1H), 2.55 (m, 1H), 2.50 (m, 1H), 2.48 (m, 1H), 2.45 (bs, 1H), 2.42 (bs, 1H), 2.41−2.34 (m, 2H), 2.31 (m, 1H), 2.26 (bs, 1H), 2.22 (m, 3H), 2.18−2.12 (m, 3H), 2.11−2.06 (m, 3H), 2.05 (s, 1H), 2.04 and 2.03 (s, s, 3H), 1.97 (m, 1H), 1.94 and 1.90 (s, s, 3H), 1.87−1.79 (m, 2H), 1.71−1.60 (m, 3H), 1.58 and 1.56 (s, s, 3H), 1.44 and 1.44 (s, s, 3H), 1.33 (s, 3H), 1.30 (m, 1H), 1.20 (s, 3H), 1.04 and 1.02 (s, s, 3H), 0.98 and 0.98 (s, s, 3H), −4.12 (s, 2H). ^{13}C NMR (125 MHz, $CDCl_3$) δ (ppm): 175.9, 175.8, 175.3, 174.3, 173.8, 173.5, 173.4, 173.2, 172.8, 172.5, 171.8, 171.6, 171.3, 170.4, 163.3, 161.6, 136.3, 130.2, 120.7, 106.1, 102.2, 97.8, 97.2, 96.9, 96.2, 91.2, 82.6, 74.6, 69.1, 68.6, 63.6, 58.3, 57.7, 56.7, 53.3, 52.4, 51.83, 51.82, 51.59, 51.57, 50.9, 46.8, 46.4, 46.0, 41.6, 39.14, 39.05, 37.2, 36.9, 33.6, 32.3, 31.6, 31.2, 30.7, 29.6, 25.7, 25.6, 24.8, 22.3, 21.9, 21.8, 21.7, 19.6, 19.2, 18.1, 16.9, 15.3, 15.0, 12.7, 11.57, 11.55.

Hybrid ***25b***. Following the procedure described above for **25a**, hybrid **24b** (66 mg, 0.04 mmol) was treated with TFA, giving hybrid **25b** as a brownish solid (46 mg, 73% yield). R_f 0.4 (5% MeOH in DCM). Anal. Calcd for $C_{93}H_{117}CoN_{12}O_{18} + 2H_2O$: C 61.31, H 6.92, N 9.23. Found: C 61.67, H 6.85, N, 9.12. HRMS ESI (m/z): calcd for $C_{92}H_{117}CoN_{11}O_{18}$ $[M - CN]^+$ 1722.7905, found 1722.7904. UV/vis (CH_2Cl_2), λ_{max} (nm) (ε, $L \cdot m^{-1} \cdot cm^{-1}$): 630 ($5.14 \times 10^3$), 584 ($1.43 \times 10^4$), 542 ($1.75 \times 10^4$), 506 ($1.72 \times 10^4$), 407 ($1.46 \times 10^5$). Regardless of the solvent used, ^{1}H and ^{13}C NMR spectra were very broad thus impossible to decipher.

Hybrid ***25c***. Following the procedure described above for **25a**, hybrid **24c** (52 mg, 0.027 mmol) was treated with TFA, giving hybrid **25c** as a brownish solid (36 mg, 74% yield). R_f 0.3 (5% MeOH in DCM). Anal. Calcd for $C_{97}H_{125}CoN_{12}O_{19} + 2H_2O$: C 63.32, H 6.96, N 9.13. Found: C 63.39, H 7.01, N, 8.91. HRMS ESI (m/z) calcd for $C_{97}H_{125}CoN_{12}O_{19}Na_2$ $[M + 2Na]^{2+}$ 933.4150, found 933.4122. UV/vis (CH_2Cl_2), λ_{max} nm (ε, $L \cdot m^{-1} \cdot cm^{-1}$): 630 ($5.34 \times 10^3$), 578 ($1.47 \times 10^4$), 541 ($1.88 \times 10^4$), 506 ($1.86 \times 10^4$), 407 ($1.59 \times 10^5$). ^{1}H NMR (500 MHz, $CDCl_3$, 303 K) δ (ppm): 9.93 (s, 0.5H), 9.84 and 9.83 (s, s, 1H), 9.79 (s, 1.5H), 9.76 (s, 0.5H), 9.58 (s, 0.5H), 8.11 (m, 2H), 7.19 (m, 2H), 6.82 (m, 2H), 6.28 (m, 2H), 6.13 (m, 2H), 5.03 and 5.02 (s, s, 1H), 4.25 (m, 2H), 4.09 (m, 2H), 3.69 (s, 3H), 3.66 (s, 3H), 3.63 (s, 3H), 3.59 (s, 6H), 3.57 (s, 3H), 3.53 (s, 6H), 3.50 (s, 3H), 3.36 and 3.31 (s,s, 3H), 3.25 (m, 2H), 3.14 (bs, 6H), 3.08 (m, 4H), 2.94 (m, 4H), 2.88 (bs, 2H), 2.82 (bs, 2H), 2.70 (m, 3H), 2.48 (m, 2H), 2.46 (m, 1H), 2.43 (m, 1H), 2.36−2.29 (m, 3H), 2.21 (m, 1H), 2.13 (m, 2H), 2.07 (m, 2H), 1.98 (m, 2H), 1.93 (s, 3H), 1.90 and 1.89 (s, s, 3H), 1.82 (m, 2H), 1.65 (m, 1H), 1.58 (m, 2H), 1.55−1.47 (m, 4H), 1.42 (m, 2H), 1.38 (s, 3H), 1.30 and 1.28 (s, s, 3H), 1.27 (s, 3H), 1.17 (m, 2H), 1.10 (s, 3H), 1.01 (s, 3H), 0.89 (s, 3H), −4.44 (s, 2H). ^{13}C NMR (125 MHz, $CDCl_3$) δ (ppm): 175.8, 175.6, 175.5, 175.2, 173.8, 173.5, 173.3, 172.8, 172.5, 171.6, 171.4, 171.2, 169.8, 163.3, 161.5, 156.3, 130.2, 129.4, 120.4, 120.0, 115.3, 105.9, 102.0, 97.4, 96.7, 91.0, 82.5, 74.5, 69.8, 69.6, 69.1, 68.6, 68.5, 58.3, 57.5, 56.4, 53.3, 52.3, 51.81, 51.77, 51.6, 51.5, 50.7, 46.6, 45.9, 41.6, 39.6, 39.1, 37.5, 37.1, 36.8, 33.6, 32.2, 31.6, 31.1, 30.6, 30.5, 29.5, 28.9, 28.4, 25.5, 25.4, 24.7, 22.6, 22.0, 21.9, 19.4, 18.8, 18.1, 16.8, 15.2, 15.1, 12.6, 12.5, 11.6, 11.5.

Hybrid ***25d***. Following the procedure described above for **25a**, hybrid **24d** (64 mg, 0.03 mmol) was treated with TFA, giving hybrid **25d** as a brownish solid (42 mg, 71% yield). R_f 0.4 (5% MeOH in DCM). Anal. Calcd for $C_{97}H_{125}CoN_{12}O_{16} + 2H_2O$: C 64.36, H 7.18, N 9.29. Found: C 64.25, H 7.13, N, 9.11. LRMS ESI (m/z): calcd for $C_{96}H_{125}CoN_{11}O_{16}Na_2$ $[M - CN]^+$ 1746.9, found 1746.8. UV/vis (CH_2Cl_2), λ_{max} (nm) (ε, $L \cdot m^{-1} \cdot cm^{-1}$): 630 ($5.68 \times 10^3$), 580 ($1.58 \times 10^4$), 542 ($2.00 \times 10^4$), 506 ($1.98 \times 10^4$), 407 ($1.70 \times 10^5$). Regardless of the solvent used, ^{1}H and ^{13}C NMR spectra were very broad thus impossible to decipher.

Purification of Recombinant Human sGC Enzyme. Recombinant human sGC enzyme was purified as described previously from Sf9 cells infected with baculoviruses expressing α1 and β1 sGC subunits. Only preparations with NO-induced activity >5 μmol/min/mg were used for the present studies.

To generate truncated sGC variants, the open reading frames coding the residues 269−690 of the α1 subunit or the residues 200−619 of the β1 subunit were cloned into the transfer vector pBacPak9 (Clontech, Mountain View, CA) to obtain the pBacPak-α1Δ269 and the pBacPak-β1Δ200 plasmids, respectively. A hexahistidine tag was also inserted at the C-terminus of the $\alpha\Delta$269 variant by PCR mutagenesis. Using these plasmids and the linearized baculovirus DNA (BaculoGold from Pharmingen, San Diego, CA), the baculoviruses expressing the truncated $\alpha\Delta$269 or $\beta\Delta$200 sGC were generated according to the manufacturer's protocol. These viruses were used to coinfect Sf9 cells to generate the truncated α1CATβ1CAT sGC variant, which was purified using the same approach as for wild-type sGC.

Heme Depletion of sGC. For experiments with heme depleted sGC, we used a previously described protocol (14) with minor modifications. In short, purified sGC was incubated with 0.2% Tween 20 for 20 min at room temperature before adding it into the reaction mixture. The final concentration of Tween 20 was no more than 0.005%, which does not affect the sGC activity.

Assay of sGC Activity in Vitro. Enzymatic activity was assayed using [α-^{32}P]GTP to [^{32}P] cGMP conversion assay as described previously[28] in buffer (0.1 mL) containing TEA (25 mM), pH 7.5, BSA (1 mg/mL), DTT (1 mM), cGMP (1 mM), $MgCl_2$ (4 mM), creatine phosphokinase (0.05 mg/mL), and creatine phosphate (5 mM). To evaluate the effect of building blocks or hybrid compounds on sGC activity, the buffer containing sGC (0.1 μg) was incubated for 10 min at room temperature with indicated concentration of the compound. The reaction was initiated by adding GTP (1 mM)/[α-^{32}P]GTP (~150000 cpm) and incubated at 37 °C for 10 min. For experiments with heme depleted sGC, we preincubated purified sGC with 0.2% Tween 20 for 20 min at room temperature before adding it into the reaction mixture.[28] The reaction was stopped by zinc acetate (400 μL of 100 mM) followed by sodium carbonate (500 μL of 120 mM). Unreacted GTP was precipitated by centrifugation and the supernatant containing cGMP was loaded onto a 2 mL of Al_2O_3. cGMP was eluted with Tris pH 7.5 (10 mL of 50 mM), and the amount of generated cGMP was calculated based on the Cherenkov counts in a β scintillation counter.

Statistical Analysis. Activity results are expressed as mean ± SD, unless indicated otherwise. Nonlinear regression and calculation of EC_{50} was performed using GraphPad Prism (GraphPad Software).

Structural Modeling. Structure model of β1 sGC HNOX domain was generated using SWISS-MODEL[29] in the automated protein structure homology-modeling regime based on the PDB 2O09, the structure of homologous HNOX protein from Nostoc sp PC7120.[23] The resulting model was visualized using the RasTop2.2 molecular visualization software.

■ ASSOCIATED CONTENT

Ⓢ Supporting Information

^{1}H and ^{13}C NMR spectra for all new compounds. This material is available free of charge via the Internet at http://pubs.acs.org.

■ AUTHOR INFORMATION

Corresponding Authors

*For D.G.: phone, +48 22 343 2051; fax, +48 22 632 6681; email, dorota.gryko@icho.edu.pl.

*For E.M.: phone, 713 486 2441; fax, 713 486 0450; email, emil.martin@uth.tmc.edu.

Author Contributions

The manuscript was written through contributions of all authors. All authors have given approval to the final version of the manuscript.

Notes

The authors declare no competing financial interest.

■ ACKNOWLEDGMENTS

This work was supported by the European Regional Development Found with the TEAM program, grant no. TEAM/2009-3/4 (D.G.) and NIH 5R01HL088128 (E.M.) and Grant-in-Aid, 12GRNT11930007 (E.M.).

■ ABBREVIATIONS USED

PpIX, protoporphyrin IX; CuAAC, copper catalyzed azide−alkyne 1,3 dipolar cycloaddition; sGC, soluble guanylyl cyclase; GTP, guanosine triphosphate; cGMP, 5′-3′ cyclic guanosine monophosphate; PAS, Per, Amt, and Sim proteins structural domain; HNOX, heme-nitric oxide/oxygen binding domain; CAT, catalytic domain; CC, coiled coil region; EDC, 1-ethyl-3-(3-dimethylaminopropyl)carbodiimide; DMAP, 4-dimethylaminopyridine; $(CN)_2$Cby, dicyanocobyrinic acid; $(CN)_2$Cbi, dicyanocobinamide; DML, designed multiple ligand; TEA, triethanolamine; BSA, bovine serum albumin; DTT, dithiothreitol

■ REFERENCES

(1) Derbyshire, E. R.; Marletta, M. A. Structure and Regulation of Soluble Guanylate Cyclase. *Annu. Rev. Biochem.* **2012**, *81*, 533−559.

(2) Russwurm, M.; Koesling, D. Isoforms of NO-sensitive guanylyl cyclase. *Mol. Cell. Biochem.* **2002**, *230*, 159−164.

(3) Ma, X.; Sayed, N.; Baskaran, P.; Beuve, A.; van den Akker, F. PAS-mediated Dimerization of Soluble Guanylyl Cyclase Revealed by Signal Transduction Histidine Kinase Domain Crystal Structure. *J. Biol. Chem.* **2008**, *283*, 1167−1178.

(4) Fritz, B. G.; Roberts, S. A.; Ahmed, A.; Breci, L.; Li, W.; Weichsel, A.; Brailey, J. L.; Wysocki, V. H.; Tama, F.; Montfort, W. R. Molecular Model of a Soluble Guanylyl Cyclase Fragment Determined by Small-Angle X-ray Scattering and Chemical Cross-Linking. *Biochemistry* **2013**, *52*, 1568−1582.

(5) Winger, J. A.; Marletta, M. A. Expression and Characterization of the Catalytic Domains of Soluble Guanylate Cyclase: Interaction with the Heme Domain. *Biochemistry* **2005**, *44*, 4083−4090.

(6) Murad, F. Nitric Oxide and Cyclic GMP in Cell Signaling and Drug Development. *N. Engl. J. Med.* **2006**, *355*, 2003−2011.

(7) Vita, J. A. Endothelial Function. *Circulation* **2011**, *124*, 906−912.

(8) Munzel, T.; Daiber, A.; Gori, T. Nitrate Therapy: New Aspects Concerning Molecular Action and Tolerance. *Circulation* **2011**, *123*, 2132−2144.

(9) Stasch, J. P.; Pacher, P.; Evgenov, O. V. Soluble Guanylate Cyclase as an Emerging Therapeutic Target in Cardiopulmonary Disease. *Circulation* **2011**, *123*, 2263−2273.

(10) ó Proinsias, K.; Giedyk, M.; Sharina, I.; Martin, E.; Gryko, D. Synthesis of New Hydrophilic and Hydrophobic Cobinamides as NO-Independent sGC Activators. *ACS Med. Chem. Lett.* **2012**, *3*, 476−479.

(11) Sharina, I.; Sobolevsky, M.; Doursout, M. F.; Gryko, D.; Martin, E. Cobinamides Are Novel Coactivators of Nitric Oxide Receptor That Target Soluble Guanylyl Cyclase Catalytic Domain. *J. Pharmacol. Exp. Ther.* **2011**, *340*, 723−732.

(12) Chromiński, M.; ó Proinsias, K.; Martin, E.; Gryko, D. Protoporphyrin IX/Cobyrinate Derived Hybrids—Novel Activators of Soluble Guanylyl Cyclase. *Eur. J. Org. Chem.* **2013**, *8*, 1530−1537.

(13) (a) Rostovtsev, V. V.; Green, L. G.; Fokin, V. V.; Sharpless, K. B. A Stepwise Huisgen Cycloaddition Process: Copper(I)-Catalyzed Regioselective "Ligation" of Azides and Terminal Alkynes. *Angew. Chem.* **2002**, *114*, 2708−2711. (b) Shao, C.; Cheng, G.; Su, D.; Xu, J.; Wang, X.; Hu, Y. Copper(I) Acetate: A Structurally Simple but Highly Efficient Dinuclear Catalyst for Copper-Catalyzed Azide−Alkyne Cycloaddition. *Adv. Synth. Catal.* **2010**, *352*, 1587−1592. (c) Tornùe, Ch. W.; Meldal, M. Cu-catalyzed azide−alkyne cycloaddition. *Chem. Rev.* **2008**, *108*, 2952−3015. (d) Bock, V. D.; Himestra, H.; van Maarseveen, J. H. Cu(I)-Catalyzed Alkyne−Azide "Click" Cycloadditions from a Mechanistic and Synthetic Perspective. *Eur. J. Org. Chem.* **2006**, 51−68. (e) Moses, J. E.; Moorhouse, A. D. The Growing Application of Click Chemistry. *Chem. Soc. Rev.* **2007**, *36*, 1249−1262. (f) Jewett, J. C.; Bertozzi, C. R. Cu-Free Click Cycloaddition Reactions in Chemical Biology. *Chem. Soc. Rev.* **2010**, *39*, 1272−1279. (g) Dumoulin, F.; Ahsen, V. Click Chemistry: The Emerging Role of the Azide−Alkyne Huisgen Dipolar Addition in the Preparation of Substituted Tetrapyrrolic Derivatives. *J. Porphyrins Phthalocyanines* **2011**, *15*, 486−504.

(14) (a) Pfammatter, M. J.; Dabre, T.; Keese, R. Synthesis of Vitamin-B_{12} Derivatives with Peripheral Tris(oxyethylene) Chains. *Helv. Chim. Acta* **1998**, *81*, 1105−1116. (b) Brown, K. L. The Chemistry and Enzymology of Vitamin B_{12}. *Chem. Rev.* **2005**, *105*, 2075−2150.

(15) Shimakoshi, H.; Tokunaga, M.; Kuroiwa, K.; Kimizuka, N.; Hisaeda, Y. Preparation and Electrochemical Behaviour of Hydrophobic Vitamin B_{12} Covalently Immobilized onto Platinum Electrode. *Chem. Commun.* **2004**, 50−51.

(16) (a) Sieber, P. Der 2-Trimethylsilyläthyl-Rest als selektiv abspaltbare Carboxy-Schutzgruppe. *Helv. Chim. Acta* **1977**, *60*, 2711−2716. (b) Back, T. G.; Wulff, A. Stereodivergent Synthesis of Virantmycin by an Enzyme-Mediated Diester Desymmetrization and a Highly Hindered Aryl Amination. *Angew. Chem Int. Ed.* **2004**, *43*, 6493−6496.

(17) (a) ó Proinsias, K.; Kurcoń, S.; Gryko, D. Hydrophobic Vitamin B_{12} Derivatives: Unprecedented Formation of a 7-Membered Lactam. *Eur. J. Org. Chem.* **2012**, 154−159. (b) Grossauer, A.; Heise, K.-P.; Götze, H.; Inhoffen, H. H. Derivate des Dicyano-cobrinsäure-hexamethylester-c-lactons. *Justus Liebigs Ann. Chem.* **1977**, 1480−1499. (c) Shimakoshi, H.; Inaoka, T.; Hisaeda, Y. Solid−solid Synthesis of a Hydrophobic Vitamin B_{12} Having a Benzo-18-crown-6 moiety at the C10 Position of the Corrin Ring. *Tetrahedron Lett.* **2003**, *44*, 6421−6424.

(18) ó Proinsias, K.; Giedyk, M.; Banach, Ł.; Rutkowska-Zbik, D.; Gryko, D. Selectively Modified Cobyrinic Acid Derivatives. *Asian J. Org. Chem.* **2013**, *2*, 504−513.

(19) (a) Morphy, R.; Rankovic, Z. Designed Multiple Ligands. An Emerging Drug Discovery Paradigm. *J. Med. Chem.* **2005**, *48*, 6524−6543. (b) Morphy, R.; Rankovic, Z. The Physiological Challenges of Designing Multiple Ligands. *J. Med. Chem.* **2006**, *49*, 4961−4970.

(20) Martin, E.; Sharina, I.; Kots, A.; Murad, F. A Constitutively Activated Mutant of Human Soluble Guanylyl Cyclase (sGC): Implication for the Mechanism of sGC Activation. *Proc. Natl. Acad. Sci. U. S. A.* **2003**, *100*, 9208−9213.

(21) Foerster, J.; Harteneck, C.; Malkewitz, J.; Schultz, G.; Koesling, D. A Functional Heme-Binding Site of Soluble Guanylyl Cyclase Requires Intact N-Termini of α1 and β1 Subunits. *Eur. J. Biochem.* **1996**, *240*, 380−386.

(22) Ignarro, L. J.; Wood, K. S.; Wolin, M. S. Activation of Purified Soluble Guanylate Cyclase by Protoporphyrin IX. *Proc. Natl. Acad. Sci. U. S. A.* **1982**, *79*, 2870−2873.

(23) Ma, X.; Sayed, N.; Beuve, A.; van den Akker, F. NO and CO differentially Activate Soluble Guanylyl Cyclase via a Heme Pivot-Bend Mechanism. *EMBO J.* **2007**, *26*, 578−588.

(24) Baskaran, P.; Heckler, E. J.; van den Akker, F.; Beuve, A. Aspartate 102 in the Heme Domain of Soluble Guanylyl Cyclase Has a Key Role in NO Activation. *Biochemistry* **2011**, *50*, 4291−4297.

(25) Martin, F.; Baskaran, P.; Ma, X.; Dunten, P. W.; Schaefer, M.; Stasch, J. P.; Beuve, A.; van den Akker, F. Structure of Cinaciguat (BAY 58−2667) Bound to Nostoc H-NOX Domain Reveals Insights into Heme-Mimetic Activation of the Soluble Guanylyl Cyclase. *J. Biol. Chem.* **2010**, *285*, 22651−22657.

(26) Allerston, C. K.; von Delft, F.; Gileadi, O. Crystal Structures of the Catalytic Domain of Human Soluble Guanylate Cyclase. *PLoS One* **2013**, *8*, e57644.

(27) ó. Proinsias, K.; Gryko, D. T.; Hisaeda, Y.; Martin, E.; Sessler, J. L.; Gryko, D. Vitamin B_{12} Derivatives as Activators of Soluble Guanylyl Cyclase. *J. Med. Chem.* **2012**, *55*, 8943−8947.
(28) Martin, E.; Lee, Y. C.; Murad, F. YC-1 Activation of Human Soluble Guanylyl Cyclase Has Both Heme-Dependent and Heme-Independent Components. *Proc. Natl. Acad. Sci. U. S. A.* **2001**, *98*, 12938−12942.
(29) Arnold, K.; Bordoli, L.; Kopp, J.; Schwede, T. The SWISS-MODEL Workspace: A Web-Based Environment for Protein Structure Homology Modelling. *Bioinformatics* **2006**, *22*, 195−201.